Supporting Information Appendix

Characterization of Glutamyl-tRNA Dependent Dehydratases using Non-Reactive Substrate Mimics

Ian R. Bothwell[1,§], Dillon P. Cogan[2,§], Terry Kim[1], Christopher J. Reinhardt[1], Wilfred A. van der Donk[1-3]*, and Satish K. Nair[1,2,4*]

Departments of [1]Chemistry and [2]Biochemistry, the [3]Howard Hughes Medical Institute, and the [4]Center for Biophysics and Computational Biology, University of Illinois at Urbana-Champaign, Roger Adams Laboratory, 600 S. Mathews Ave., Urbana, Illinois 61801, United States.

[§] These authors contributed equally to this work.

Table of contents:

Materials and Methods

General materials and methods

Unless otherwise noted, general chemical reagents and solvents were purchased from MilliporeSigma (Burlington, MA) or Fischer Scientific (Hampton, NH) and used as provided. Silica 60M (0.04-0.063 mm) was purchased from Machery-Nagel (Düren, DE).

www.pnas.org/cgi/doi/10.1073/pnas.1905240116

Standard Fmoc- and Boc-protected L-amino acids were purchased from Chem-Impex International (Wood Dale, IL) or Advanced ChemTech (Louisville, KY). Preloaded Fmoc-L-Lys(Boc) Wang resin, Fmoc-Dap(Alloc)-OH, and 2-(6-chloro-1-H-benzotriazole-1-yl)-1,1,3,3-tetramethylaminium hexafluorophosphate (HCTU) were purchased from Chem-Impex International. Oligonucleotides and enzymes/buffers used for molecular biology/cloning were purchased through Integrated DNA Technologies Inc. (Coralville, IA; SI Appendix Tables 3-4) or New England Biolabs, respectively (Ipswich, MA). Plasmid isolation was accomplished using QIAprep spin columns according to the manufacturer instructions (Qiagen, DE). Sequencing services were procured through ACGT Inc. (Wheeling, IL). MALDI–TOF MS analysis was performed at the University of Illinois Mass Spectrometry Facility using a Bruker UltrafleXtreme MALDI–TOF/TOF mass spectrometer (Billerica, Massachusetts) in reflector mode. All samples were purified by C18 ZipTip® (MilliporeSigma) prior to being cospotted 1:1 (*v/v*) with 50 mg/mL "super"-DHB (9:1 w/w 2,5-dihydroxybenzoic acid and 2-hydroxy-5-methoxybenzoic acid) as matrix. Mass spectrometry data were exported and analyzed using mMass software (1). NMR spectra were collected using a Varian Unity 400 MHz or Bruker 500 MHz spectrometer equipped with a CryoProbe and data were analyzed using Mnova software (Mestrelab Research, S.L., ES).

Enzyme and Peptide Purification:

Cloning and heterologous TbtB protein expression

Plasmids encoding WT TbtB or site-directed mutants for heterologous protein expression in *E. coli* were constructed using the pET hexahis (His_6)-small ubiquitin-like modifier (SUMO)-tobacco etch virus (TEV) protease ligation-independent cloning (LIC) vector (2S-T). This vector was a gift from Scott Gradia (Addgene plasmid #29711). Mutations were generated via PCR using primers containing the LICv1 cloning tags (SI Appendix Table 3) and ligated into SspI-treated 2S-T via Gibson Assembly (2). The resulting His_6-SUMO-TbtB encoding plasmids were propagated in *E. coli* DH5α for plasmid isolation, and sequence-verified plasmids were used to transform *E. coli* Rosetta (DE3) competent cells for protein expression. Transformants were used to inoculate 50 mL or 4 L (for downstream activity or structural applications, respectively) of Luria-Broth (LB)

medium and cells were grown at 37 °C with shaking (220 rpm) until an optical density at 600 (OD_{600}) of 0.4-0.6 was achieved. The cells were then cooled in an ice bath for 15 min and protein expression was induced by the addition of 0.5 mM isopropyl β-D-1-thiogalactopyranoside (IPTG) and further incubated at 18 °C with shaking (220 rpm) for 20 h.

Generation of NisB glutamylation/elimination domain mutants

Alanine mutants in the glutamylation and elimination domains of NisB were generated using site-directed, ligation-independent mutagenesis (SLIM) on a pRSF-Duet1 template containing His_6-tagged NisA in MCSI and NisB in MCSII (3). Primers used for this process are included in SI Appendix Table 4 and denoted as F_t, F_s, R_t, and R_s in accordance with original reports for the procedure (4). Following amplification, PCR products were digested with DpnI to remove template. Appropriate combinations of PCR products were then mixed and rehybridized prior to transformation of DH5α cells and growth on LB agar plates containing kanamycin (LB^{kan}). Plasmid DNA was obtained from overnight liquid cultures using a miniprep kit (Qiagen, DE) and mutant incorporation was confirmed by sequencing. Mutant constructs were then used to transform BL21 Star (DE3) cells plated on LB^{Kan} agar for subsequent coexpression and NisA purification (see below).

Purification of NisA peptide coexpressed with NisB mutants:

E. coli BL21 Star (DE3) colonies containing the mutant plasmids described above were used to inoculate 5 mL overnight starter cultures in LB^{Kan}. A portion of these cultures (500 µL) was used to inoculate 100 mL of LB expression cultures, which were incubated at 37 °C with shaking until they reached an OD_{600} of approximately 0.6. At this point, cultures were cooled on ice for 30 min prior to the addition of IPTG to a final concentration of 0.5 mM. Cultures were placed back into an incubator set to 18 °C and allowed to shake overnight (220 rpm). Cells were harvested by centrifugation of the culture media at 4,500 × g for 15 min, decanted, and stored at −80 °C. Purification of NisA was performed as described previously (5) with minor alteration. Notably, peptide purifications were small in scale (1 mL buffer volumes) using Micro Bio-Spin™ columns (Bio-Rad Laboratories, CA) and His60 Ni Superflow Resin (200 µL resin bed volume; Takara Bio Inc., JP) in

accordance with manufacturer instructions. Product peptides were desalted by C18 ZipTip® (MilliporeSigma) prior to MALDI-TOF MS analysis.

EF-Tu purification

Escherichia coli JM109/pKECA-Tu (6, 7) producing C-terminally His_6-tagged EF-Tu was a generous gift from the laboratory of Dr. Michael Ibba (Ohio State University, Columbus, OH). Expression cultures (2 L, LB) containing 100 μg/mL ampicillin (Amp) were inoculated from 5 mL overnight starter cultures and grown at 37 °C to an OD_{600} of 0.6. Expression was induced by addition of IPTG to a final concentration of 0.5 mM. Cultures were shaken at 37 °C for 6 h before being harvested by centrifugation at 4,500 × g. Cells were rinsed once with 0.1 M Tris HCl pH 8.0 before being pelleted and resuspended in lysis buffer (25 mM Tris HCl pH 7.5, 300 mM NaCl, 10 μM GDP, 5 mM imidazole and 10 % glycerol). Cells were lysed using an Avestin C3 homogenizer (ATA Scientific) and the lysate clarified by centrifugation at 23,000 × g at 4 °C for 25 min. The clarified lysate was loaded onto an equilibrated nickel-nitrilotriacetic (Ni-NTA) column attached to an ÄKTA FLPC system (GE Healthcare), washed with lysis buffer and then eluted using a gradient of elution buffer (Elution Buffer B: 50 mM Tris HCl pH 7.6, 10 mM $MgSO_4$, 2.5 mM TCEP, 50 mM NH_4Cl, 10 μM GDP, 500 mM imidazole, 10% glycerol; 1.5 mL/min, 0% B 30 mins, 10 % B over 20 mins, 100% B over 10 mins). Desired fractions were pooled and dialyzed overnight against 1 L of dialysis buffer (50 mM Tris HCl pH 7.6, 10 mM $MgSO_4$, 2.5 mM TCEP, 50 mM NH_4Cl, 10 μM GDP, and 10% glycerol). Lastly, dialyzed EF-Tu was concentrated using a 10K cutoff Amicon centrifugal filter (EMD Millipore) and stored at −80 °C prior to use.

His_6-SUMO-TbtB wild type and site-directed variants

Cells were harvested by centrifugation at 3,000 × g and cell pellets were suspended in 25 mL of buffer A (0.5 M NaCl, 10% glycerol (*v/v*), and 20 mM Tris-HCl pH 8.0). Suspended cells were lysed via sonication and the lysate was cleared by centrifugation at 15,400 × g for 1 h at 4 °C. Supernatant was applied to 2 mL of HisPur Ni-NTA resin (Thermo Scientific) by gravity elution. The resin was washed with 40 mL of buffer B (1 M NaCl, 30 mM imidazole, and 20 mM Tris-HCl pH 8.0) prior to eluting the protein with

buffer C (1 M NaCl, 0.1 M imidazole, and 20 mM Tris-HCl pH 8.0) in 1 mL increments for 2 total fractions followed by buffer D (1 M NaCl, 0.5 M imidazole, and 20 mM Tris-HCl pH 8.0) in 1 mL increments for eight total fractions. Proteins at this point appeared ≥95% pure by sodium dodecyl sulfate polyacrylamide gel electrophoresis (SDS-PAGE) (SI Appendix Figure 5).

His_6-TbtB

Cells were harvested and lysed as described for the His_6-SUMO-TbtB variants. Supernatant was injected onto a 5 mL Ni-NTA HisTrap HP column (GE Healthcare) equilibrated with buffer A using an ÄKTA purifier. The column was washed with 50 mL of buffer B followed by a linear gradient elution of 0-100% buffer D over 40 mL (2 mL/min). Thrombin protease was added (1 U/mg substrate; Millipore Sigma) to elution fractions to remove the His_6-tag while dialyzing into 0.3 M NaCl, 3 mM β-mercaptoethanol (BME), 20 mM Tris-HCl pH 8.0 for 12 h. Dialysis was repeated in a similar buffer lacking BME for another 4 h before injecting protein onto a Ni-NTA HisTrap HP column (GE Healthcare) equilibrated with buffer A for subtractive Ni-affinity purification. The column was washed with 40 mL of buffer A before eluting with a stepwise gradient of increasing buffer B (i.e., 5, 10, 15, 20, 25, 30, 50, and 100 %B). Increments of 5 mL were used between each step unless a peak was observed by absorbance at 280 nm, in which case, the % B composition was maintained for the entire peak elution. The majority of tag-free TbtB protein eluted between 15-25% B as monitored by SDS-PAGE. Pooled fractions of tag-free TbtB were concentrated to ≤5 mL and injected onto a 120 mL Superdex 200 10/300 GL column (GE Healthcare) to purify the protein by size-exclusion chromatography (SEC) using 300 mM KCl, 20 mM 4-(2-hydroxylethyl)-1-piperazineethanesulfonic acid (HEPES) pH 7.5 as running buffer. TbtB eluted as a monomer and appeared ≥90% pure by SDS-PAGE (SI Appendix Figure 5).

Preparation of SeMet-NisB-V169C

SeMet-derivatized NisB-V169C (SM-NisB-V169C) was generated using similar growth conditions to TbtB variants with substitution of LB medium for M9 minimal medium (0.4% (*w/v*) glucose, 11.2 g/L $Na_2HPO_4{\cdot}7H_2O$, 3 g/L KH_2PO_4, 1 g/L NH_4Cl, 0.12

g/L $MgSO_4$, and 0.5 g/L NaCl) supplemented with 4.2 mg/L $FeSO_4$, 0.5 mg/L thiamine hydrochloride, 0.1 g/L L-Lys, 0.1 g/L L-Phe, 0.1 g/L-Thr, 50 mg/L L-Leu, 50 mg/L L-Ile, 50 mg/L L-Val, and 50 mg/L L-SeMet.

Cells were harvested, lysed, and protein from the supernatant was purified by Ni-affinity chromatography as described for His_6-TbtB. Pooled fractions of SM-NisB-V169C were used to methylate surface exposed Lys residues following reported procedures (8). The reductive amination reaction was quenched by addition of 0.1 M Tris pH 7.5, and the protein was further purified by SEC as described for TbtB. Methylated SM-NisB-V169C eluted as a dimer and appeared ≥90% pure by SDS-PAGE (SI Appendix Figure 5).

Protein crystallization:

TbtB: TbtB purified by SEC was concentrated to 2 mg/mL prior to crystallization in 2 µL hanging drops by mixing (1:1; *v/v*) protein and reservoir solution (0.2 M ammonium citrate pH 7.0 and 15.0% polyethylene glycol (PEG) 3350) and incubating at 20 °C. Ellipsoid-shaped crystals grew to maximum size within a week.

TbtB+PDG (soak): Drops containing apo TbtB crystals were supplemented with 10 mM PDG (dissolved in H_2O) and incubated for 8 h at 20 °C.

SM-NisB-V169C+NisA-Ser3Dap^{Glu}: Methylated SM-NisB-V169C purified by SEC was concentrated to 9 mg/mL and incubated with 2 equiv. NisA-Ser3Dap^{Glu} (150 µM) for 30 min on ice. The covalent complex was crystallized in 2 µL hanging drops by mixing (1:1; *v/v*) protein and reservoir solution (18.3% PEG 6000, 0.1 M bicine pH 8.0, and 1 mM dithiothreitol (DTT)) and incubating at 9 °C. Hexagonal-shaped crystals grew to maximum size in 72 h. Under these conditions the RRE-peptide disulfide linkage does not appear to be reduced in the crystals, on the basis of electron density (SI Appendix Figure 11A).

X-ray diffraction data collection and structure solution

Crystals were cryoprotected prior to data collection by brief immersion in reservoir solutions supplemented with 20% ethylene glycol prior to vitrification by immersion into liquid nitrogen. Data were collected at sector 21 of the Advanced Photon Source (Argonne

National Laboratory) using the Life Science Collaborative Access Team (LS-CAT) 21-ID-D, 21-ID-F, and 21-ID-G beamlines. An MD2 diffractometer (Arinax Scientific Instrumentation) was used for crystal mounting and 100 K temperature maintenance under an aerosolized nitrogen stream. TbtB crystals were soaked with 10 mM thiomersal for 8 h at room temperature prior to cryoprotection and data were collected at the mercury absorption edge (12.35 keV) to obtain anomalous signal for phasing. Data were processed using XDS and autoPROC to obtain structure factors, and phases were determined by the single-wavelength anomalous diffraction technique implemented in Phenix AutoSol (9-11). The initial TbtB model was rebuilt in Phenix AutoBuild and refined using Phenix Refine and REFMAC5 with additional manual refining in Coot (12-15). Diffraction data for SM-NisB-V169C crystals were collected at 12.67 keV and structure factors were scaled using autoPROC. Phases were determined by molecular replacement using the NisB coordinates previously reported (PDB 4WD9) in Phaser MR (16). The protein coordinates were refined in a similar fashion to TbtB. Ligand parameters for PDG and residue NisA-Ser3Dap^{Glu} were generated by creating a structure-data file (sdf) in ChemDraw Professional 17.1. The sdf file was input into Phenix eLBOW, and the output cif and pdb files were used in refinement (17).

Additional Experimental Procedures:

Analysis of TbtB mutant activity:

The activity assays involving purified His_6-SUMO-TbtB mutants were conducted without removal of the SUMO tag and in accordance with previous reports (18). In brief, 10 μL reactions were prepared containing 5 μM TbtB variant, 5 μM TbtC, 10 μM *T. bispora* GluRS, 10 μM *T. bispora* tRNA^{Glu}, and 100 μM TbtA hexazole in TbtB reaction buffer (150 mM KCl, 5 mM $MgCl_2$, 5 mM ATP, 10 mM glutamate, and 100 mM HEPES pH 7.5). Reactions proceeded at room temperature for 1 h prior to desalting using C18 ZipTip® (MilliporeSigma) and analysis by MALDI-TOF MS. Wild-type TbtB and no-enzyme samples were included as controls.

Synthesis of PDG

PDG was synthesized starting from 3′-azido-3′-deoxyadenosine (**1**, *SI Appendix* Scheme 1), prepared from 3′-azido-3′deoxy-2′,5′-bis-*O*-(tert-butyldimethylsilyl)-adenosine according to previous reports (19). Following reduction of the 3′-azide to the corresponding amine, coupling of Boc/tBu-protected glutamate was achieved through reaction with Boc-Glu(OtBu)-OSu to afford compound **2**. Selective protection of the 5′-OH with *tert*-butyldiphenylsilyl chloride (TBDPS-Cl), followed by benzoylation of adenine at *N*-6 and *C*-2′-OH with benzoyl chloride (BzCl) yielded compounds **3** and **4**, respectively. Removal of the 5′-TBDPS group with tetrabutylammonium fluoride (TBAF) yielded a suitable substrate (**5**) for chemical phosphorylation, which was achieved through coupling to bis(2-cyanoethyl)-*N,N*-diisopropylphosphoramidite followed by *in situ* oxidation of the resulting phosphite triester using *t*-butyl hydroperoxide to afford **6**. Treatment of this compound with ethanolic ammonium hydroxide resulted in the removal of cyanoethyl and benzoyl protecting groups. Lastly, treatment with trifluoroacetic acid (TFA) produced the final product (**7**), which was purified by reversed-phase HPLC.

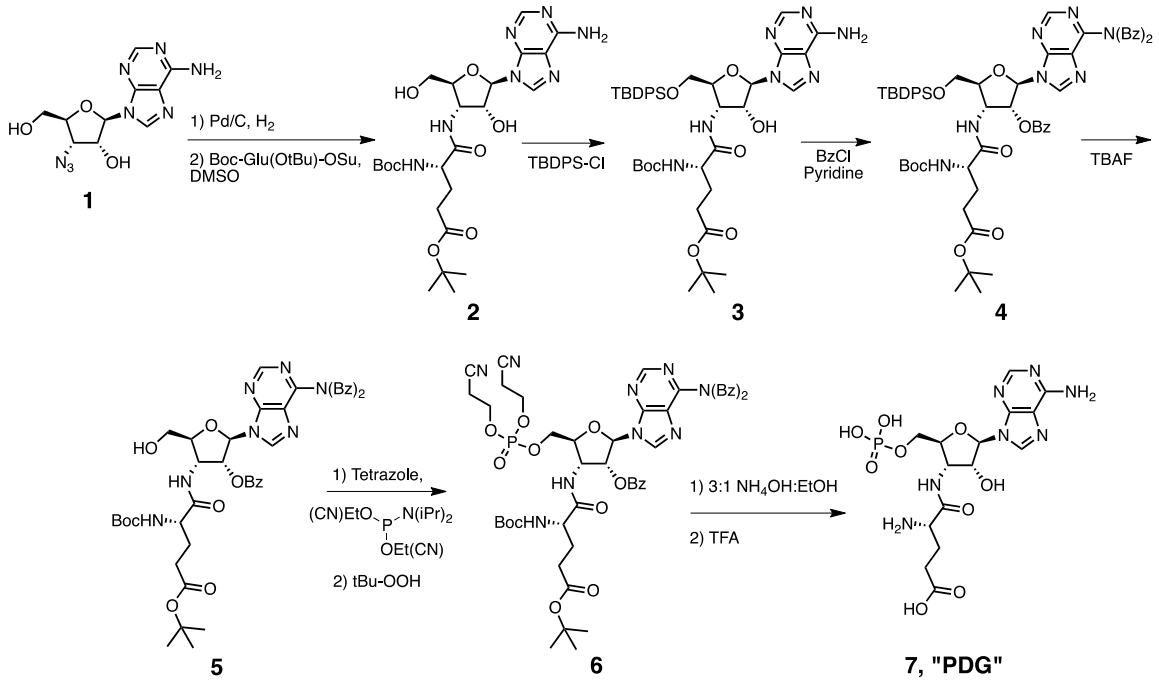

SI Appendix Scheme 1: Synthesis of PDG.

Synthesis of compound **2**:

3′-Azido-3′-deoxyadenosine (**1**; 40 mg; 137 μmol), prepared according to established methods (19), was dissolved in a 1:1 1,4-dioxane:MeOH mixture containing 10% acetic acid (3 mL). Palladium on carbon (10 weight %; 4 mg) was added and the reaction vessel flushed with H_2. The reaction was allowed to proceed under H_2 for 8 h with vigorous stirring. Reaction progress was monitored by TLC using 9:1 dichloromethane (DCM):MeOH as mobile phase. Following complete transformation, the reaction was filtered through Celite, the solvent was removed by rotary evaporation, and the residue was dried under reduced pressure to yield 57 mg of crude product. This crude product was used without further purification for the coupling reaction. Briefly, the intermediate product was dissolved in 1.5 mL of anhydrous dimethylsulfoxide (DMSO) and placed under N_2 atmosphere. To the solution was added Boc-Glu(OtBu)-OSu (106 mg; 266 μmol; 1.3 equiv.) and the reaction was allowed to proceed for 8 h at room temperature. Water (1 mL) was added and the reaction was stirred for 30 min. The product mixture was then placed in a heated speedvac (55 °C) to remove the DMSO/H_2O mixture. The brown residue was suspended in a minimum amount of 19:1 DCM:MeOH and purified by flash chromatography over silica gel (19:1 DCM:MeOH mobile phase) to afford the product (30 mg; 56 μmol; 37% yield). **^{1}H NMR (500 MHz, $CDCl_3$):** δ ppm 8.15 (s, 1H, H2), 7.89 (s, 1H, H8), 5.90 (1H, H1'), 4.74 (1H, H2'), 4.65 (1H, Hα), 4.37 (1H, H3'), 4.19 (1H, H4'), 3.87 (dm, J = 90 Hz, 2H, H5'), 2.36 (m, 2H, Hγ), 2.015 (dm, J = 85 Hz, 2H, Hβ), 1.41-1.38 (18H, tBu). **^{13}C NMR (125 MHz, $CDCl_3$):** δ ppm 174.18, 173.62, 156.37, 155.61, 152.20, 147.88, 139.83, 119.57, 91.26, 85.19, 81.03, 80.35, 73.76, 61.77, 54.23, 50.89, 32.03, 29.90, 29.58, 29.30. LR-ESI-MS (m/z): calculated for $C_{24}H_{37}N_7O_8$ = 551.27, observed $[M+H]^+$ 552.3.

Synthesis of compound **3**:

Compound **2** (30 mg; 56 μmol) was dissolved in 2 mL of anhydrous pyridine and the reaction vessel flushed with nitrogen. DMAP (8.4 mg; 67.2 μmol) and TBDPS-Cl (112.6 μL; 432 μmol; ~8 equiv.) were then added. The reaction was allowed to proceed at room temperature for 48 h at room temperature with stirring. Methanol (0.5 mL) was added and the reaction allowed to proceed an additional 30 min before the removal of solvent by

rotary evaporation. The resulting residue was taken up in 150 mL of $CHCl_3$ and washed with water (2x 25 mL), saturated sodium bicarbonate (2x 25 mL), and brine (3x 25 mL). Aqueous phases were back-extracted with $CHCl_3$ (2x 25 mL) and the combined organic phases were dried over sodium sulfate. Solvent was removed by rotary evaporation and the crude product purified by silica gel flash chromatography using 19:1 DCM:MeOH as the mobile phase. Appropriate fractions were pooled and solvent was removed by rotary evaporation to afford the product (38 mg; 48.2 μmol; 87% yield). **^{1}H NMR (500 MHz, $CDCl_3$)**: δ ppm 8.22 (s, 1H, H2), 8.13 (s, 1H, H8), 7.62 (d, J =10 Hz, 4H, arom.), 7.36-7.32 (m, 6H, arom.), 6.01 (d, J = 2.5 Hz, 1H, H1'), 5.56 (m, 1H, H2'), 4.62 (d, J = 5.5 Hz, 1H, Hα), 4.25 (m, 1H, H3'), 4.16 (m, 1H, H4'), 3.91 (dd, J_a = 85.5 Hz, J_b = 11 Hz, 2H, H5'), 2.35-2.26 (m, 2H, Hγ), 2.02-1.89 (m, 2H, Hβ), 1.41 (s, 9H, tBu), 1.38 (s, 9H, tBu), 1.00 (s, 9H, Si-tBu). **^{13}C NMR (125 MHz, $CDCl_3$):** δ ppm 172.69, 172.65, 156.16, 155.83, 152.74, 148.86, 138.74, 135.89, 135.65, 133.08, 132.80, 130.05, 129.99, 129.0, 127.96, 120.07, 91.13, 84.37, 81.15, 80.46, 74.86, 63.35, 53.63, 50.82, 50.64, 32.0, 29.9, 28.50, 28.28, 27.78, 27.05, 19.37. LR-ESI-MS (m/z): calculated for $C_{40}H_{55}N_7O_8Si$ = 789.39, observed $[M+H]^+$ 790.4.

Synthesis of compound **4**:

Compound **3** (38 mg; 48.2 μmol) was dissolved in 2 mL of anhydrous pyridine under nitrogen and placed in a 4 °C ice bath. To this solution was added benzoyl chloride (57 μL; 490 μmol; 10 equiv.) divided in three 19 μL portions. The reaction was allowed to stir on ice for 1 h then brought to room temperature overnight. Water (0.5 mL) was added and the reaction allowed to stir for 1 h at room temperature. Solvent was removed by rotary evaporation and the residue was taken up in 150 mL of ethyl acetate then washed with water (2x 25 mL), saturated sodium bicarbonate (2x 25 mL), and brine (3x 25 mL). The organic phase was dried over sodium sulfate and removed by rotary evaporation. The crude residue was purified by silica gel flash chromatography using 1:1 ethyl acetate: hexanes as the mobile phase. Appropriate fractions were pooled and evaporated to dryness to afford the product (52 mg; 47.2 μmol; 98% yield). **^{1}H NMR (500 MHz, $CDCl_3$):** δ ppm 8.49 (s, 1H, C2-H), 8.22 (s, 1H, C8-H), 8.01 (d, J_a = 8.5 Hz, 2H, arom.), 7.79 (d, J_a = 7 Hz, 4H, arom.), 7.54 (m, 6H, arom.), 7.40 (dt, J_a = 4.5 Hz, J_b = 7.5 Hz, 4H, arom.), 7.27 (m, 8H,

arom.), 7.19 (m, 3H, arom.), 6.23 (d, J_a = 3 Hz, 1H, H1') 5.81 (dd, J_a = 6.5 Hz, J_b = 4 Hz, 1H), 5.32 (dt, J_a = 6.5 Hz, J_b = 8.5 Hz, 1H, H2'), 5.16 (d, J_a = 7.5 Hz, 1H), 4.24 (m, 1H, Hα), 3.96-3.85 (m, 2H, H5'), 2.22 (dm, J_a = 93 Hz, 2H, Hγ), 1.8 (dm, J_a = 52.5 Hz, 2H, Hβ), 1.35 (s, 9H, tBu), 1.23 (s, 9H, tBu), 0.97 (s, 9H, tBu). **^{13}C NMR (125 MHz, $CDCl_3$):** δ ppm 173.25, 172.44, 171.94, 171.35, 165.43, 152.66, 152.56, 152.08, 143.75, 135.88, 135.70, 134.26, 134.09, 133.11, 132.74, 130.24, 130.06, 129.88, 129.65, 128.92, 128.85, 128.78, 128.04, 127.95, 127.88, 88.52, 84.17, 81.34, 76.42, 63.58, 60.59, 49.81, 32.17, 29.89, 28.35, 28.23, 27.05, 21.24, 19.38, 14.39. LR-ESI-MS (m/z): calculated for $C_{61}H_{67}N_7O_{11}Si$ 1101.47, observed $[M+H]^+$ 1102.5.

Synthesis of compound **5**:

Compound **4** (20 mg; 18.2 μmol) was dissolved in anhydrous THF and the solution cooled on ice under nitrogen. To this solution was added a 1 M solution of TBAF in THF (20 μL) and the reaction was monitored by analytical TLC using 3:2 ethyl acetate: hexanes as the mobile phase. After 3 h, the solvent was removed by rotary evaporation. The residue was taken up in 150 mL of ethyl acetate and washed with saturated sodium bicarbonate (5x 20 mL) and once with brine. The organic phase was then dried over sodium sulfate and solvent was removed. Crude product was then purified by silica gel flash chromatography using 3:2 ethyl acetate: hexanes as the mobile phase. Combined product fractions yielded 12 mg (13.9 μmol; 76% yield) of product. **^{1}H NMR (500 MHz, $CDCl_3$):** δ ppm 8.65 (s, 1H, C2-H), 8.42 (s, 1H, C8-H), 8.04 (d, J = 5 Hz, 2H, arom.), 7.83 (d, J = 5 Hz, 4H, arom.), 7.46 (m, 4H, arom.), 7.34 (t, J = 10 Hz, 4H, arom.), 6.34 (d, J = 3 Hz, 1H, NH), 5.81 (dd, J_a = 6.5 Hz, J_b = 3.5 Hz, 1H, H1'), 5.29 (d, J = 7.5 Hz, 1H), 5.12 (dd, $J_{a,b}$ = 6.5 Hz, 1H, H2'), 4.36-433 (m, 2H, Hα, H3'), 3.95 (dm, J = 115 Hz, 2H, H5'), 2.32 (dm, J_a, = 95 Hz, 2H, Hγ), 1.77 (dm, J_a = 80 Hz, 2H, Hβ), 1.39 (s, 9H, tBu), 1.29 (s, 9H, tBu). **^{13}C NMR (125 MHz, $CDCl_3$):** δ ppm 173.23, 173.16, 172.42, 165.42, 152.47, 152.36, 152.28, 144.21, 134.24, 134.12, 133.26, 130.26, 129.69, 129.00, 128.89, 128.59, 128.39, 89.55, 84.87, 81.52, 76.64, 61.72, 60.62, 49.97, 36.84, 32.14, 28.35, 28.24, 24.89, 21.27. LR-ESI-MS (m/z): calculated for $C_{45}H_{49}N_7O_{11}$ = 863.91, observed $[M+H]^+$ 864.4.

Synthesis of compound **6**:

Under dry conditions, compound **5** (22 mg; 25.5 μmol) was dissolved in 1 mL of anhydrous acetonitrile. To this solution was added 1H-tetrazole (446 μL of 0.45 M solution in anhydrous acetonitrile; 204 μmol; 8 equiv.) and bis(2-cyanoethyl)-*N,N*-diisopropylphosphoramidite (13.11 μL; 51 μmol; 2 equiv.). The reaction was allowed to proceed at room temperature for 3 h and then analyzed by TLC using a 9:1 DCM:MeOH mobile phase. After confirming complete consumption of the starting material, the phosphite triester was oxidized *in situ* through treatment with 20 μL of *t*-butyl hydroperoxide solution (6 M solution in decane) for 30 min. The reaction was then dried by rotary evaporation and the product taken up in 150 mL of ethyl acetate. This solution was then washed with 15 mL of water, 15 mL of saturated sodium bicarbonate, and 15 mL of brine (2x each). Aqueous phases were pooled and back-extracted once with ethyl acetate. The combined organic phases were then dried over sodium sulfate followed by rotary evaporation. The crude product was purified by silica gel flash chromatography using 3% MeOH:DCM as the mobile phase. Combined product fractions yielded 20 mg of material (19 μmol; 76% yield). **^{1}H NMR (500 MHz, $CDCl_3$):** δ ppm 8.67 (s, 1H, C2-H), 8.27 (s, 1H, C8-H), 8.11 (d, J = 8 Hz, 2H, arom.), 7.84 (d, J = 8 Hz, 4H, arom.), 7.49 (t, J = 7.5 Hz, 4H, arom.), 7.36 (t, J = 8 Hz, 5H, arom.), 6.26 (br, 1H, NH), 5.95 (d, J_a = 6 Hz, 1H, H1'), 5.53 (dd, J_a = 6 Hz, J_b = 9 Hz, 1H, H2'), 5.26 (br, 1H, NH), 4.52 (m, 1H, H3'), 4.45 (m, 1H, Hα), 4.39 (m, 1H, H4'), 4.26-4.08 (m, 6H, C5' and cyanoethyl), 2.67 (m, 4H, cyanoethyl), 2.39 (dm, J = 65 Hz, 2H, Hγ), 1.97 (dm, J = 75 Hz, 2H, Hβ), 1.39 (s, 9H, tBu), 1.27 (s, 9H, tBu). **^{13}C NMR (125 MHz, $CDCl_3$):** δ ppm 173.32, 172.56, 172.48, 152.72, 152.51, 152.37, 144.18, 134.42, 134.13, 133.38, 130.39, 129.72, 129.09, 129.01, 128.03, 116.92, 116.84, 89.28, 85.85, 81.44, 76.60, 62.75, 62.03, 60.52, 58.07, 46.61, 46.27, 32.22, 30.08, 30.05, 28.39, 28.29, 23.89, 22.75, 22.56, 19.91. LR-ESI-MS (m/z): calculated for $C_{51}H_{56}N_9O_{14}P$ = 1049.37, observed $[M+H]^+$ 1050.3.

Synthesis of 5′-phosphoryl-desmethylglutamycin ("PDG", **7**):

Compound **6** (17 mg; 16.2 μmol) was suspended in a freshly prepared solution of 3:1 NH_4OH:EtOH (3 mL) and the solution was allowed to stir at room temperature overnight. Bulk solvent was removed by rotary evaporation, with a small portion set aside

for comparison to fully deprotected product by HPLC/MS. The resulting residue was dissolved in 2 mL of neat TFA and kept on ice for 30 min. Bulk TFA was then removed by rotary evaporation and the residue placed under vacuum. This crude product was dissolved in water and purified by C18 reversed phase HPLC, (analytical Machery-Nagel C18; Solvent A: water containing 0.1% TFA; Solvent B: acetonitrile containing 0.1% TFA; 1 mL/min linear gradient 0-100% B over 20 min) affording the final product, which was lyophilized and dissolved in water prior to storage at −20 °C. Yield was determined by UV absorption at 256 nm using the molar extinction coefficient for adenosine (15,400 cm^{-1} mol^{-1}) and found to be 3.37 mg (7.1 μmol, 43.8% yield). **^{1}H NMR (500 MHz, D_2O):** δ ppm 8.64 (s, 1H, arom.), 8.45 (s, 1H, arom.), 6.27 (d, J = 2 Hz, 1H, H1') 4.86 (m, 1H, H2'), 4.50 (m, 1H, H4'), 4.19 (ddm, J_a = 102.5 Hz, J_b = 12 Hz, 1H, H5'), 4.07 (t, J = 6.5 Hz, 1H, Hα), 2.61 (t, J = 7 Hz, 2H, Hγ), 2.24 (q, J = 7 Hz, 2H, Hβ). **^{13}C NMR (125 MHz, D_2O):** δ ppm 176.01, 169.69, 149.89, 147.88, 144.45, 142.38, 118.77, 90.12, 81.02, 73.62, 63.59, 52.55, 51.00, 29.08, 25.71. HR-MS (m/z): calculated for $C_{15}H_{23}N_7O_9P$ = 476.1295, observed 476.1275

Solid-phase peptide synthesis of NisA-Ser3Dap^{Glu}

Automated peptide synthesis was performed on a 0.1 mM scale using a Rainin PS3 synthesizer. Coupling reactions were performed using 4 equiv. of the appropriate Fmoc-amino acid and 4 equiv. of HCTU dissolved in dimethylformamide (DMF) containing 0.4 M *N*-methylmorpholine. Deprotection steps were carried out using 20% piperidine in DMF. Double-couplings were performed for residues following proline. The progress of the synthesis was periodically monitored by MALDI-TOF MS after cleavage/deprotection of a small amount of resin. The linear protected NisA truncant was first prepared according to the sequence: Boc-S^{tBu}-T^{tBu}-K^{Boc}-D^{tBu}-F-N^{Trt}-L-D^{tBu}-L-V-C^{Trt}-V-S^{tBu}-K^{Boc}-K^{Boc}-D^{tBu}-S^{tBu}-G-A-S^{tBu}-P-R^{Pbf}-I-T^{tBu}-Dap^{Alloc}-I-S^{tBu}-L-A-T^{tBu}-P-G-A-K^{Boc} – Wang Resin (SI Appendix Scheme 2A). Upon completion, the resin-bound product was removed from the synthesizer, washed, and dried. From this point on, all remaining steps were performed manually. Selective deprotection of the Ser3Dap^{Alloc} residue was achieved by first swelling the resin in DCM under a N_2 atmosphere. Phenylsilane (2.0 mM; 20 equiv.) dissolved in 2 mL of DCM was then added to the resin, followed by an additional 2 mL of DCM

containing $Pd(PPh_3)_4$ (0.035 mM; 0.35 equiv.). The reaction was stirred gently for 20 min using a magnetic stirrer at room temperature before draining the solution and washing the resin with DCM (5x 10 mL). The entire process was repeated to ensure removal of the Alloc group.

Coupling of Boc-Glu(OtBu)-OH to the newly liberated amine of the Dap residue was accomplished by treating swollen resin with 5 mL of DMF solution containing 0.4 M *N*-methylmorpholine, 0.4 mM Boc-Glu(OtBu)-OH, and 0.4 mM HCTU. The coupling reaction was gently stirred for 45 min using a magnetic stirrer at room temperature before draining the solution and washing the resin with DMF (5x 10 mL). This process was repeated once more to ensure complete coupling before rinsing the resin with DCM and drying. Side chain deprotection and cleavage from resin was accomplished by treating ~100 mg of resin-bound peptide with 1 mL of cleavage cocktail composed of 38:1:1 TFA:H_2O:TIPS for 1 h at room temperature. The resulting solution was then filtered through glass wool before precipitating the peptide product in 10 mL of ice-cold diethyl ether. The peptide was pelleted by centrifugation and washed with 10 mL of diethyl ether three times prior to drying overnight. Dried peptide pellet was dissolved in 10 mL of H_2O containing 0.1% TFA before being purified by C18 reversed phase HPLC. Product fractions were confirmed by MALDI-TOF MS prior to being combined and lyophilized. The resulting peptide product was dissolved in water containing 0.1% TFA and stored at −20 °C prior to use.

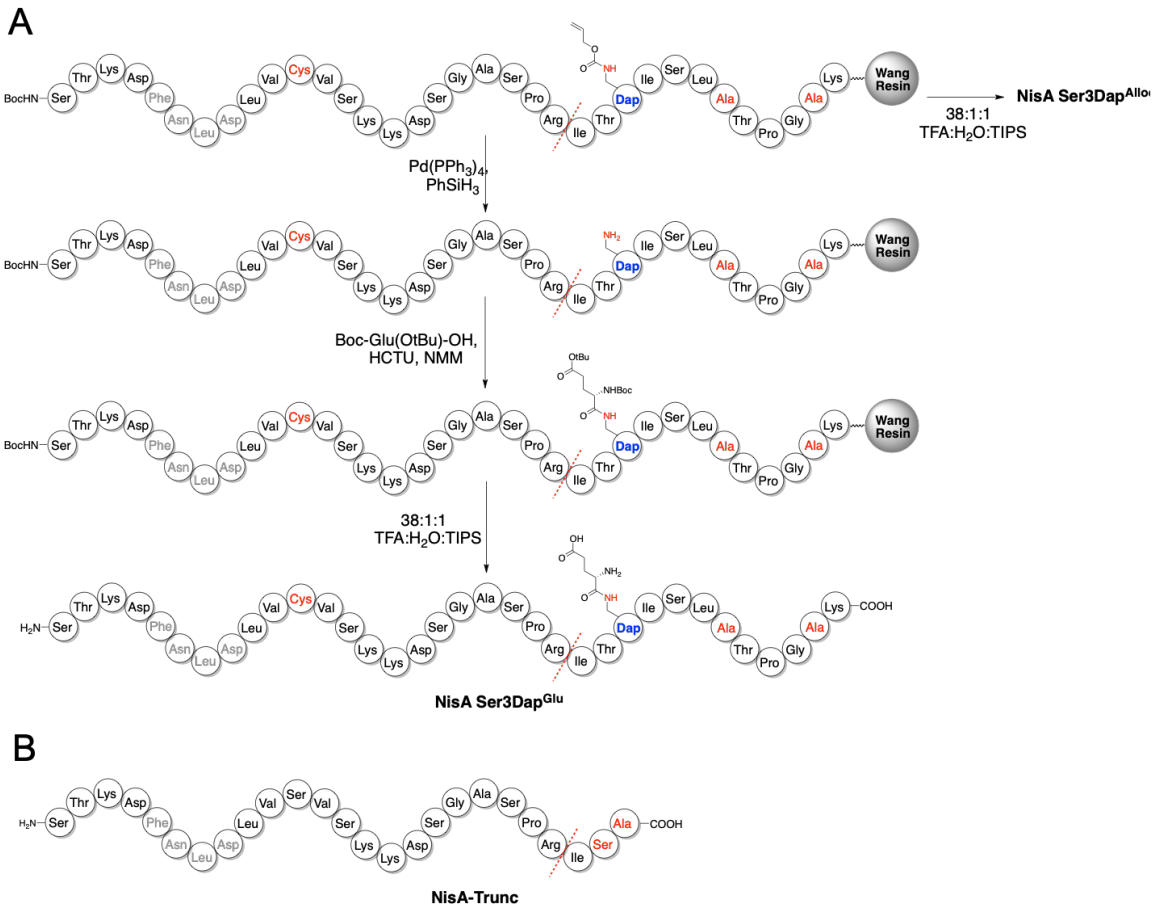

SI Appendix Scheme 2: Preparation of the NisA-Ser3Dap^{Glu} substrate mimic and NisA-Trunc peptide. (A) NisA-Ser3Dap^{Glu} was prepared via the orthogonal Alloc-protecting group strategy outlined above. The NisA-Ser3Dap^{Alloc} and NisA-Ser3Dap peptides were isolated from intermediate steps in the synthesis. The Dap residue is highlighted in blue text and Cys-to-Ala substitutions are shown in red. The FNLD motif needed for RRE interaction is shown in grey. The dashed line represents the natural proteolysis site separating the core and leader regions. (B) The truncated NisA peptide, NisA-Trunc, was synthesized according to standard Fmoc-SPPS described below. Note the Ser and Ala substitutions at positions +2 and +3 (in red) from the naturally occurring Thr and Ser, respectively.

SPPS of NisA-Trunc

Peptide synthesis was performed on a 0.1 mM scale using a CEM Liberty automated microwave peptide synthesizer (CEM Holding Corporation, Matthews, NC). Instrument stock solutions were prepared as: 0.2 M Fmoc-amino acid in DMF; 0.5 M HCTU dissolved in DMF (activator); 2 M *N,N*-diisopropylethylamine in *N*-methyl-2-pyrrolidinone (activator base); 20% piperidine in DMF containing 0.1 M HOBt (deprotection); and 0.5 M acetic anhydride, 0.125 M diisopropylethylamine (DIPEA) and 0.015 M HOBt in DMF (capping). The linear protected NisA truncant was prepared

according to the sequence: S^{tBu}-T^{tBu}-K^{Boc}-D^{tBu}-F-N^{Trt}-L-D^{tBu}-L-V-C^{Trt}-V-S^{tBu}-K^{Boc}-K^{Boc}-D^{tBu}-S^{tBu}-G-A-S^{tBu}-P-R^{Pbf}-I-S^{tBu}-A–Wang Resin (SI Appendix Scheme 2B). Upon completion, the resin-bound product was removed from the synthesizer, washed with DCM, and dried. Side chain deprotection and cleavage from resin was accomplished as needed by treating resin-bound peptide with 1 mL of cleavage cocktail composed of 38:1:1 TFA:H_2O:triisopropylsilane (TIPS) for 1 h at room temperature. The resulting solution was then filtered through glass wool before precipitating the peptide product in 10 mL of ice-cold diethyl ether. The peptide was pelleted by centrifugation and washed with 10 mL of diethyl ether three times prior to drying overnight. Dried peptide pellet was dissolved in 10 mL of H_2O containing 0.1% TFA and purified by C18 reversed phase HPLC. Product fractions were confirmed by MALDI-TOF MS prior to being combined and lyophilized. The resulting peptide product was dissolved in water containing 0.1% TFA and stored at −20 °C prior to use.

Analysis of NisB activity towards NisA substrate mimics:

The ability of NisB to dehydrate NisA mimics was examined as follows. Reactions (30 μL) were performed containing: 5 μM wild type NisB, 10 μM *E. coli* GluRS, and 20 μM *E. coli* $tRNA^{Glu}$ in NisB reaction buffer (10 mM KCl, 10 mM $MgCl_2$, 1 mM TCEP, 5 mM ATP, and 50 mM HEPES pH 7.5). The synthetic peptide mimics, NisA-Ser3Dap^{Glu} or NisA-Ser3Dap^{Alloc}, were added to a final concentration of 50 μM and the reaction allowed to proceed at room temperature. Aliquots were removed at various time points and desalted using C18 ZipTips® (MilliporeSigma) prior to MALDI-TOF MS analysis. Data from these experiments are presented in SI Appendix Figure 9.

EF-Tu competition assays with NisB

EF-Tu was charged with GTP to its active form according to the method described by Ling et al. (7). Briefly, a 310 μM stock solution of EF-Tu was activated in 50 mM HEPES pH 7.6, 50 mM KCl, 10 mM $MgSO_4$, 50 mM NH_4Cl, 5 mM phosphoenol pyruvate, 2 mM GTP, 1 mM TCEP, and 100 μg/μL pyruvate kinase for 20 min on ice. This stock solution was then diluted and added to NisB reactions containing 100 μM NisA, 10 μM *E. coli* GluRS, and 20 μM *E. coli* $tRNA^{Glu}$ in 1x NisB reaction buffer (10 mM KCl, 10 mM

$MgCl_2$, 1 mM TCEP, 5 mM ATP, and 50 mM HEPES pH 7.5). Reactions were incubated for 10 min on ice prior to the addition of NisB to a final concentration of 2.5 μM. Reactions were then allowed to proceed at room temperature for 2 h prior to desalting using C18 ZipTips® (MilliporeSigma) and analysis by MALDI-TOF MS.

Table 1: Summary of TbtB and NisB glutamylation domain residues targeted for mutagenesis and *in vitro* activity analyses in this study and in previous reports (3, 20). Relative enzyme activities are designated as inactive (-), partially active (+), or fully active (++).

TbtB	NisB	Mutation	TbtB activity	NisB activity	Reference
Arg22	Arg14	Ala	-	-	This study and Garg et al., 2013
Lys193	Lys79	Ala	insoluble	-	This study
Tyr194	Tyr80	Ala/Phe	not tested	- / -	This study and Khusainov et al., 2015
Arg197	Arg83	Ala	-	-	This study and Garg et al., 2013
Lys201	Arg87	Ala	-	-	This study and Garg et al., 2013
Thr202	Ser88	Ala	++	++	This study
Ser203	Thr89	Ala	+	-	This study and Garg et al., 2013
Tyr564	Phe435	Ala	+	not tested	This study
Gln566	Asn437	Ala	++	not tested	This study
Asn576	Asp451	Ala	++	not tested	This study
His579	Asn455	Ala	+	not tested	This study
Arg743	Pro613	Ala	++	not tested	This study
Phe783	Tyr643	Ala	++	+	This study
Arg785	Glu679	Ala	+	not tested	This study
Glu829	Gln681	Ala	++	not tested	This study
Glu851	Asp700	Ala	+	+	This study

Table 2. Sequence conservation of glutamylation domain residues in TbtB and NisB that were investigated in this study. TbtB sequence conservation (left yellow column) is expressed as a percentage on the basis of a multiple sequence alignment (MSA) of nine thiopeptide glutamylation domains (Pfam: PF04738; Lant_dehydr_N): TbtB (WP_013130810.1; thiomuracin), PbtB (WP_084779543.1; GE2270), PbtB1 (WP_068921148.1; GE2270), BC5084 (WP_000802628.1; thiocillin), NocE (ADR01081.1; nocathiacin), KocB (ATG31919.1; kocurin), CltE (WP_014677374.1; cyclothiazomycin), and two putative thiopeptide glutamylation domains WP_079128249.1 and WP_026413556.1 (21). Percentage of NisB sequence conservation (right yellow column) is according to the MSA of nine full length LanB sequences generated by Garg et al., 2013 (3). Completely conserved residues (or highly similar residue pairs) from the nine TbtB/NisB sequences were further evaluated for conservation using MSAs of 250 sequences generated using either TbtB (WP_013130810.1) or NisB (WP_014570406.1) as BLAST queries and MUSCLE (22). The left column for each protein (green) shows the percentage where the position in question is not a gap (% non-gapped) in the MSA. The right column for each protein then shows the most common amino acid at that position and its frequency (% Max AA).

		9 Sequence MSA		250 Sequence MSA			
TbtB	NisB	% Conservation (TbtB MSA)	% Conservation (NisB MSA)	% Non-gapped (TbtB MSA)	% Max AA (TbtB MSA)	% Non-gapped (NisB MSA)	% Max AA (NisB MSA)
Arg22	Arg14	100	100	90.8	99.6 R	83.2	100 R
Lys193	Lys79	56 (Lys/Arg)	78			92.8	64.7 K
Tyr194	Tyr80	100 (Tyr/Phe)	100	98.4	86.2 Y	92.8	97.8 Y
Arg197	Arg83	100	100	98.4	99.6 R	92.8	100 R
Lys201	Arg87	100	100	98.4	98.8 K	92.8	100 R
Thr202	Ser88	78	78				
Ser203	Thr89	100 (Ser/Thr)	100	98.4	98.8 S	92.8	100 T
Tyr564	Phe435	78	44 (Phe/Tyr)				
Gln566	Asn437	100	22	99.6	99.2 Q		
Asn576	Asp451	100	11	99.2	99.6 N		
His579	Asn455	56	11				
Arg743	Pro613	100	78	99.2	100 R		
Phe783	Tyr643	100 (Phe/Tyr)	56	98.8	85.4 F (14.6 Y)		
Arg785	Glu679	89	22				
Glu829	Gln681	44 (Glu/Asp)	33				
Glu851	Asp700	100	100 (Asp/Glu)	98.8	99.6 E	92.4	69.7 E (30.3 D)

Table 3: Primers used in the generation of TbtB mutant constructs.

Primer name	Sequence 5'-3'
TbtB F LICv1	TACTTCCAATCCAATGCAATGCGTCTGGTGGAACGTCGCTTTC
TbtB R LICv1	TTATCCACTTCCAATGTTATTATTATTCACCCAGTTCAACCAGAA ATTCGATCACAC
TbtB R22A F	GAAAGTCGCAGTGGCTGAATGCGGTCTGCC
TbtB R22A R	GCAGACCGCATTCAGCCACTGCGACTTTCG
TbtB K193A F	CTGCTGCGCCTGGCCGCATATGTTGCACGTGCG
TbtB K193A R	GCACGTGCAACATATGCGGCCAGGCGCAGCAGT
TbtB R197A F	CCAAATATGTTGCAGCTGCGGCCGTCAAAACG
TbtB R197A R	GTTTTGACGGCCGCAGCTGCAACATATTTGGC
TbtB K201A F	GCACGTGCGGCCGTCGCAACGTCACCGTACTC
TbtB K201A R	CGAGTACGGTGACGTTGCGACGGCCGCACGTG
TbtB T202A F	CGTGCGGCCGTCAAAGCGTCACCGTACTCGAC
TbtB T202A R	GGTCGAGTACGGTGACGCTTTGACGGCCGCAC
TbtB S203A F	GCGGCCGTCAAAACGGCACCGTACTCGACCTT
TbtB S203A R	AAAGGTCGAGTACGGTGCCGTTTTGACGGCCG
TbtB Y564A F	CGTTCTTGCGCGTGTGCTGTCCAGCCGGCACC
TbtB Y564A R	CGGTGCCGGCTGGACAGCACACGCGCAAGAAC
TbtB H579A F	GTGCTGAACGTTGTCGCTGGCGGTCACGGTCG
TbtB H579A R	ACGACCGTGACCGCCAGCGACAACGTTCAGCAC
TbtB Q566A F	TGCGCGTGTTATGTCGCGCCGGCACCGGAAGG
TbtB Q566A R	GCCTTCCGGTGCCGGCGCGACATAACACGCGC
TbtB N576A F	GGCCGCCTGGTGCTGGCCGTTGTCCATGGCGG
TbtB N576A R	ACCGCCATGGACAACGGCCAGCACCAGGCGGC
TbtB R584A F	CCATGGCGGTCACGGTGCTGGTCTGCGTCGCCT
TbtB R584A R	CAGGCGACGCAGACCAGCACCGTGACCGCCATG
TbtB R743A F	CGTGTCGTGGTTCAAGCTCGCCGTTGGCTGGCA
TbtB R743A R	GTGCCAGCCAACGGCGAGCTTGAACCACGACAC
TbtB F783A F	CATCCCGACGCGTTCAGCTGTTCGCGCCTGGC
TbtB F783A R	CTGCCAGGCGCGAACAGCTGAACGCGTCGGGA
TbtB R785A F	ACGCGTTCATTTGTTGCCGCCTGGCAGGAACG
TbtB R785A R	GCGTTCCTGCCAGGCGGCAACAAATGAACGCG
TbtB E829A F	GCATTTGTGCTGTTCGCAGAAGCTCTGCCGGA
TbtB E829A R	GTCCGGCAGAGCTTCTGCGAACAGCACAAATG
TbtB E851A R LICv1	TTATCCACTTCCAATGTTATTATTCACCCAGTTCAACCAGAAATG CGATCACACGCGGCA

Table 4: Primers used in the generation of pRSFDuet1-His_6NisA (MCSI) NisB mutant coexpression constructs via site-directed ligase-independent mutagenesis. Lowercase letters indicate overhanging regions of complementarity.

Primer name	Sequence 5'-3'
NisBbp800 SeqF	Ctcagaaatagaaattggtgaagg
NisBbp2500 SeqR	Gaatcggcacaaaatattgcttc
NisB K79A Fs	AGAAGTTATTTACGATCAACTCC
NisB K79A Ft	ctatttacgcctattataagAGAAGTTATTTACGATCAACTCC
NisB K79A Rs	ATTCAAATAATTTTTTAACCCTTTTCTTC
NisB K79A Rt	cttataataggcgtaaatagATTCAAATAATTTTTTAACCCTTTTCTTC
NisB Y80A Fs	TTATTTACGATCAACTCCATTTGG
NisB Y80A Ft	ctatttacaaggcctataagagaagTTATTTACGATCAACTCCATTTGG
NisB Y80A Rs	ATTCAAATAATTTTTTAACCCTTTTCTTC
NisB Y80A Rt	cttctcttataggccttgtaaatagATTCAAATAATTTTTTAACCCTTTTCTTC
NisB E344A Fs	TGTAGATCAAGAAGTACAAATAACAG
NisB E344A Ft	gataaatttatcgccaaatatggTGTAGATCAAGAAGTACAAATAACAG
NisB E344A Rs	CTTATAGTCATCCAAATATGTTCTTCTTAC
NisB E344A Rt	ccatatttggcgataaatttatcCTTATAGTCATCCAAATATGTTCTTCTTAC
NisB Y643A Fs	GAGATAATAAAGTTTATTTATCACAGG
NisB Y643A Ft	gagtttgccattgtcaatgGAGATAATAAAGTTTATTTATCACAGG
NisB Y643A Rs	TTTGGGAATTTCTTTGCTTTG
NisB Y643A Rt	cattgacaatggcaaactcTTTGGGAATTTCTTTGCTTTG
NisB D700A Fs	CTTTTATTAGAACGAGAGCATTAGG
NisB D700A Ft	gagagttgccgccgttgtagtgcCTTTTATTAGAACGAGAGCATTAGG
NisB D700A Rs	CCCTTTTCTCCTTTATTTATGATATTTTC
NisB D700A Rt	gcactacaacggcggcaactctcCCCTTTTCTCCTTTATTTATGATATTTTC
NisB W737A Fs	CATTGTACATTTCTATAAATCGTCAAAATG
NisB W737A Ft	ctttaacgaggccctttatctagCATTGTACATTTCTATAAATCGTCAAAATG
NisB W737A Rs	GGCAATTTTTCACGCCG
NisB W737A Rt	ctagataaagggcctcgttaaagGGCAATTTTTCACGCCG
NisB Y739A Fs	TACATTTCTATAAATCGTCAAAATG
NisB Y739A Ft	gtggcttgccctagcattgTACATTTCTATAAATCGTCAAAATG
NisB Y739A Rs	TCGTTAAAGGGCAATTTTTC
NisB Y739A Rt	caatgctagggcaagccacTCGTTAAAGGGCAATTTTTC
NisB F772A Fs	ATATACTGATCCTAAACCACATATTAG
NisB F772A Ft	ggaaatctagccttcctaagATATACTGATCCTAAACCACATATTAG
NisB F772A Rs	ACCCAGGTTTGCTACTATTTTC
NisB F772A Rt	cttaggaaggctagatttccACCCAGGTTTGCTACTATTTTC
NisB Y776A Fs	TAAACCACATATTAGATTGCGTATAAAATG
NisB Y776A Ft	cttcctaagagccactgatccTAAACCACATATTAGATTGCGTATAAAATG
NisB Y776A Rs	AATAGATTTCCACCCAGGTTTG
NisB Y776A Rt	ggatcagtggctcttaggaagAATAGATTTCCACCCAGGTTTG

NisB Y820A Fs	TAGAAAGATATGGTGGATTTGATACTTTAG
NisB Y820A Ft	gatatttctattgccgatcaagaagTAGAAAGATATGGTGGATTTGATACTTTAG
NisB Y820A Rs	AAAAGTTGACATTATCCTATTTTTCC
NisB Y820A Rt	cttcttgatcggcaatagaaatatcAAAAGTTGACATTATCCTATTTTTCC
NisB Y827A Fs	ATACTTTAGAGTTATCCGAAGC
NisB Y827A Ft	gtagaaagagccggtggatttgATACTTTAGAGTTATCCGAAGC
NisB Y827A Rs	TTCTTGATCATAAATAGAAATATCAAAAG
NisB Y827A Rt	caaatccaccggctctttctacTTCTTGATCATAAATAGAAATATCAAAAG
NisB F840A Fs	GATTCTAAAATTATTCCAAATTTGCTTAC
NisB F840A Ft	cgaagcaatagcctgtgccGATTCTAAAATTATTCCAAATTTGCTTAC
NisB F840A Rs	GATAACTCTAAAGTATCAAATCCACC
NisB F840A Rt	ggcacaggctattgcttcgGATAACTCTAAAGTATCAAATCCACC
NisB D973A Fs	AAATTAATTTATTACACACTTCAAAGG
NisB D973A Ft	gtattgaacgagccaaagagAAATTAATTTATTACACACTTCAAAGG
NisB D973A Rs	CAATTAGTCGGTTATTATGGACATG
NisB D973A Rt	ctctttggctcgttcaatacCAATTAGTCGGTTATTATGGACATG

Table 5: X-ray crystallography data collection and refinement statistics.

	TbtB	TbtB-5PG	NisB*-NisA-Ser3Dap^{Glu}
PDB ID	6EC7	6EC8	6M7Y
Data collection			
Space group	$P2_1$	$P2_1$	P 1 2_1 1
a, b, c (Å)	44.8, 96.4, 107.0	44.5, 96.1, 107.1	99.6, 107.1, 135.4
α, β, γ, (°)	90.0, 98.8, 90.0	90.0, 98.8, 90.0	90.0, 109.6, 90.0
Wavelength (Å)	0.97858	0.97872	0.97856
Resolution (Å)[1]	105.76-2.15 (2.19-2.15)	96.10-2.15 (2.19-2.15)	29.39-2.79 (2.89-2.79)
Total reflections[1]	310,750 (15,382)	309,386 (15,114)	423,377 (21,423)
Unique reflections[1]	48,860 (2,405)	48,184 (2,366)	62,066 (4,205)
R_{merge}[1]	0.065 (0.621)	0.062 (0.727)	0.090 (0.836)
$CC_{1/2}$[1]	0.999 (0.893)	0.999 (0.877)	0.998 (0.867)
I/σ(I)[1]	15.1 (2.2)	17.6 (2.1)	21.5 (2.3)
Completeness (%)[1]	100.0 (100.0)	99.1 (98.4)	93.1 (82.9)
Multiplicity[1]	6.4 (6.4)	6.4 (6.4)	6.8 (5.1)
Refinement			
Resolution (Å)[1]	105.76-2.15 (2.21-2.15)	105.80-2.15 (2.20-2.15)	29.39-2.79 (2.89-2.79)
R_{factor} (%)[1,2]	21.6 (32.0)	21.7 (33.0)	18.5 (22.8)
R_{free} (%)[1,2]	27.2 (32.9)	26.2 (30.8)	27.0 (34.5)
Number of non-hydrogen atoms	6,556	6,594	16,394
Protein	6,326	6,306	15,891
Ligands	0	32	256
Water	230	256	247
RMSD (bonds) (Å)	0.014	0.015	0.010
RMSD (angles) (Å)	1.790	1.820	1.190
Ramachandran statistics			
Favored (%)	94.0	93.0	92.0
Allowed (%)	4.9	4.6	6.5
Outliers (%)	1.5	2.5	1.7
Average B-factor (Å^2)	51.09	49.50	46.44
Macromolecules	51.08	49.54	46.39
Ligands	-	37.14	57.18
Solvent	51.46	50.11	38.55

*NisB is methylated, SeMet-derivatized, and V169C (see Methods)

1. Highest resolution shell is shown in parentheses.
2. R-factor = $\Sigma(|F_{obs}|-k|F_{calc}|)/\Sigma|F_{obs}|$ and R-free is the R value for a test set of reflections consisting of a random 5% of the diffraction data not used in refinement.

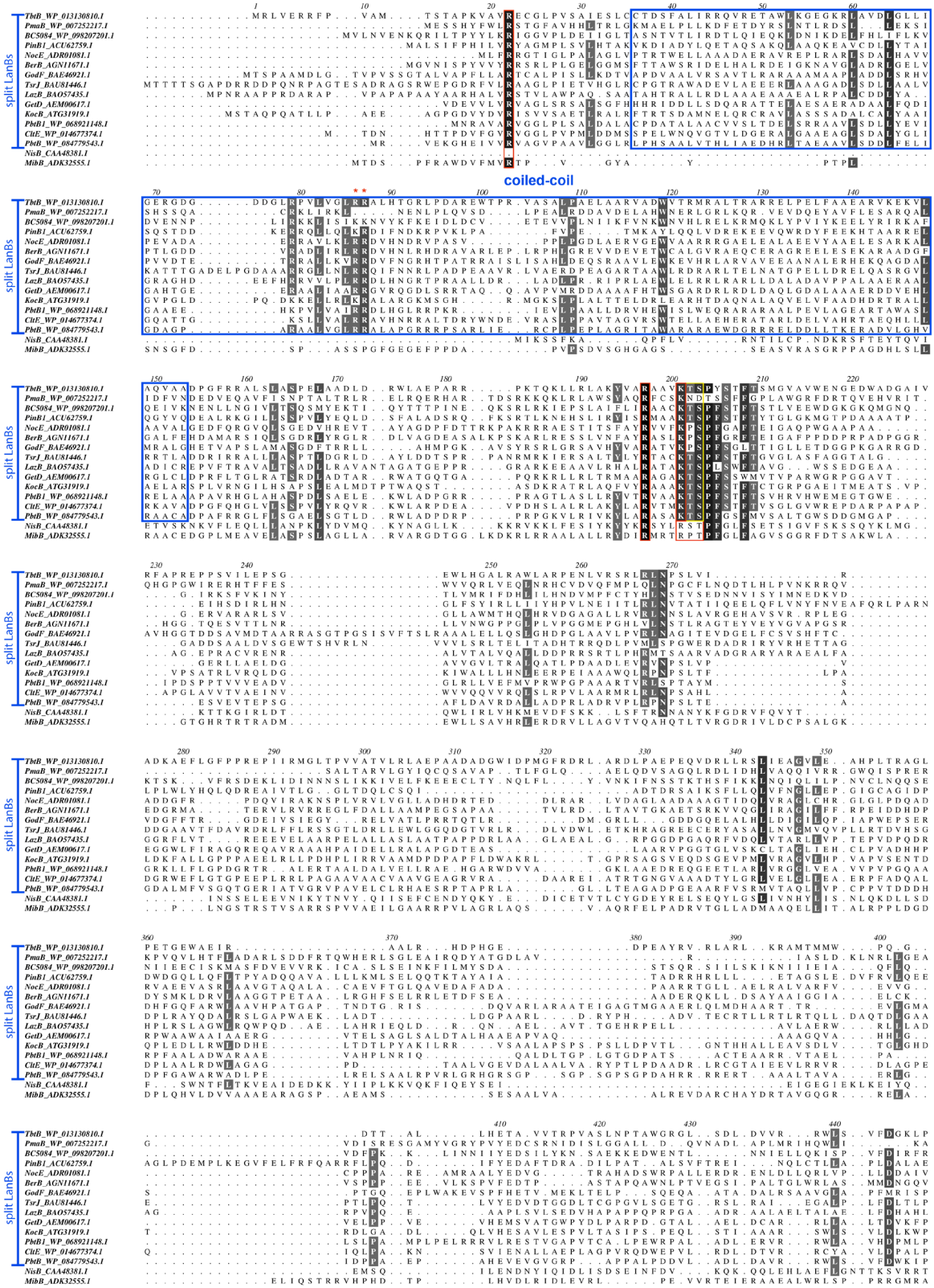
split LanBs
coiled-coil
TbtB_WP_013130810.1
PmaB_WP_007252217.1
BC5084_WP_098207201.1
PinB1_ACU62759.1
NocE_ADR01081.1
BerB_AGN11671.1
GodF_BAE46921.1
TsrJ_BAU81446.1
LazB_BAO57435.1
GetD_AEM00617.1
KocB_ATG31919.1
PhtB1_WP_068921148.1
CltE_WP_014677374.1
PhtB_WP_084779543.1
NisB_CAA48381.1
MibB_ADK32555.1

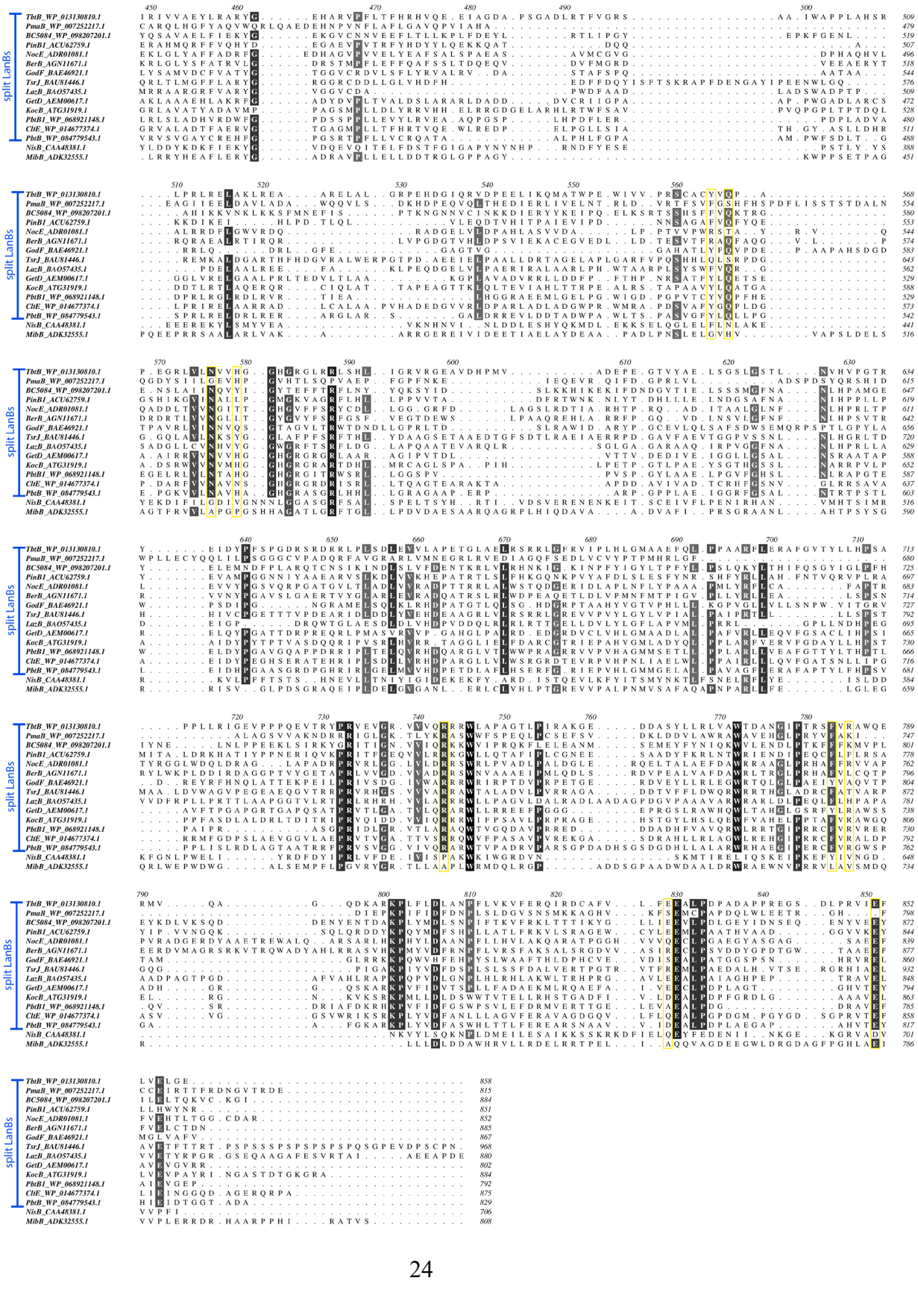
split LanBs
ThtB_WP_013130810.1
PmaB_WP_007252217.1
BC5084_WP_098207201.1
PinB1_ACU62759.1
NocE_ADR01081.1
BerB_AGN11671.1
GodF_BAE46921.1
TsrJ_BAU81446.1
LtzB_BAO57435.1
GetD_AEM00617.1
KocB_ATG31919.1
PhtB1_WP_068921148.1
CltE_WP_014677374.1
PhtB_WP_084779543.1
NisB_CAA48381.1
MibB_ADK32555.1

SI Appendix Figure 1 (previous two pages): Multiple sequence alignment of split LanBs and NisB/MibB glutamylation domains generated in Aline (8). TbtB and NisB residues (numbered according to TbtB) targeted for mutagenesis which gave partial or no impairment to activity are highlighted in yellow, and residues critical for activity are highlighted in red (associated homologous sequences are also boxed). The coiled-coil subdomain boundaries are boxed in blue for the split LanB sequences. Two Arg residues (i.e., Arg86 and Arg87) in the coiled-coil subdomain of TbtB are highlighted with a red asterisk and are conserved in 96% and 100% of 250 TbtB homologs, respectively (see SI Appendix Table 2 legend). A majority (11/14) of the stand-alone glutamylation-domain-like LanB sequences are derived from thiopeptide biosynthetic gene clusters (BGCs) with the remaining three sequences from the lanthipeptide pinensin BGC (PinB1), the linear azole-containing peptide goadsporin BGC (GodF), and the 3-thiaglutamate BGC (PmaB from *Pseudomonas syringae*) (9–11). All these enzymes have the coiled-coil subdomain even though they are in biosynthetic pathways in which they would be expected to interact with very different enzymes. Hence, if this domain is involved in protein-protein interactions with other biosynthetic enzymes, then these interactions would be conserved in a set of remarkably diverse enzymes.

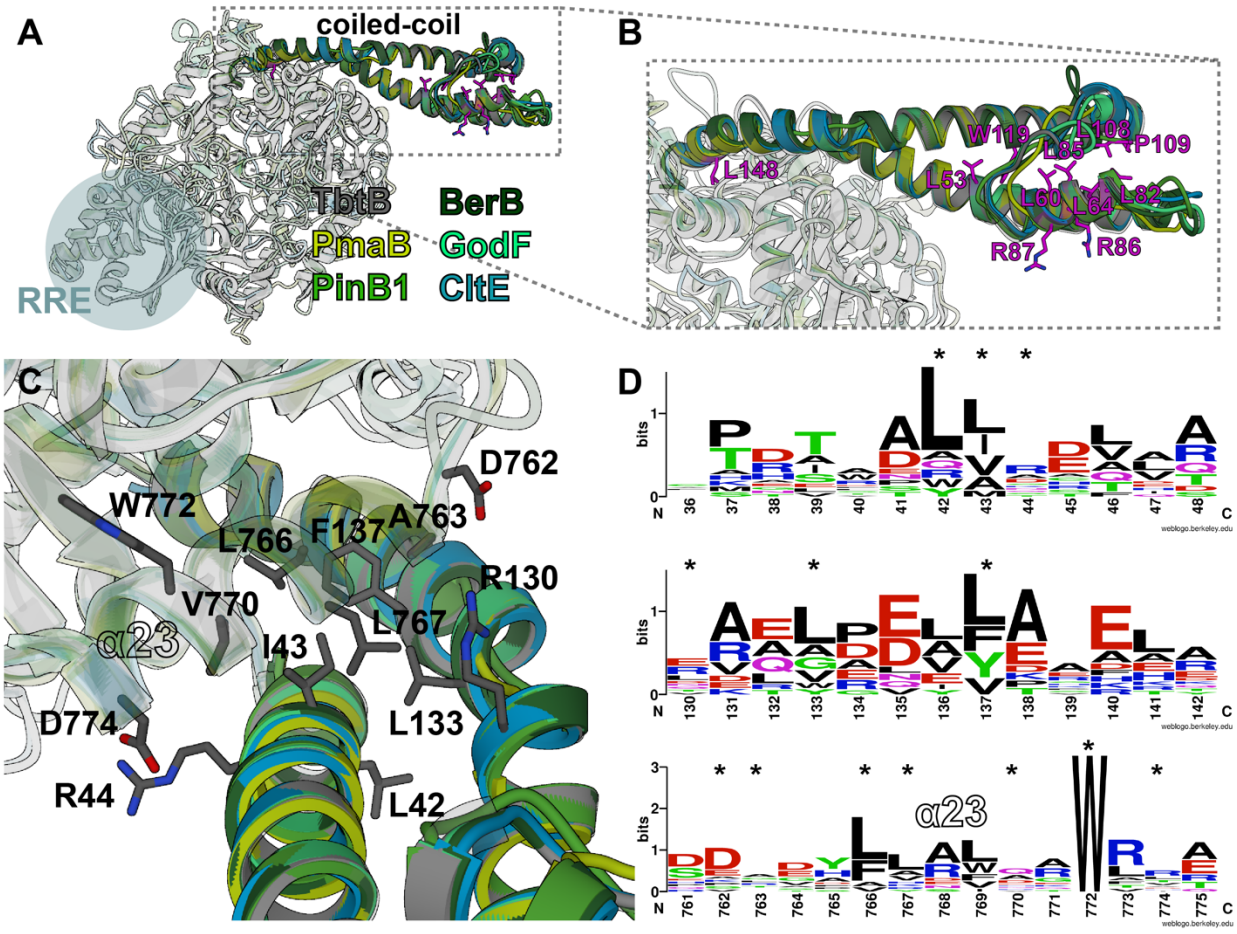

SI Appendix Figure 2: (A) Superposition of TbtB and select homology models of split (or small) LanB homologs (for accession numbers, see SI Appendix Figure 1). Homology models were generated in SWISS-MODEL using TbtB as a template (23). (B) Coiled-coil subdomain present in all aligned structures. Conserved residues in the multiple sequence alignment (SI Appendix Figure 1) are shown as magenta sticks, and the features outside of the coiled-coil subdomain are made 80% transparent for clarity. (C) Close-up view of tertiary interactions between the coiled-coil and helix α23 in TbtB. (D) Sequence logos derived from sequences in the multiple sequence alignment (save for NisB and MibB) encompassing the interaction interface between the coiled-coil and helix α23. Residue numbers correspond to the TbtB sequence (WP_013130810.1). Residue positions marked with an asterisk are shown for TbtB in panel C (24).

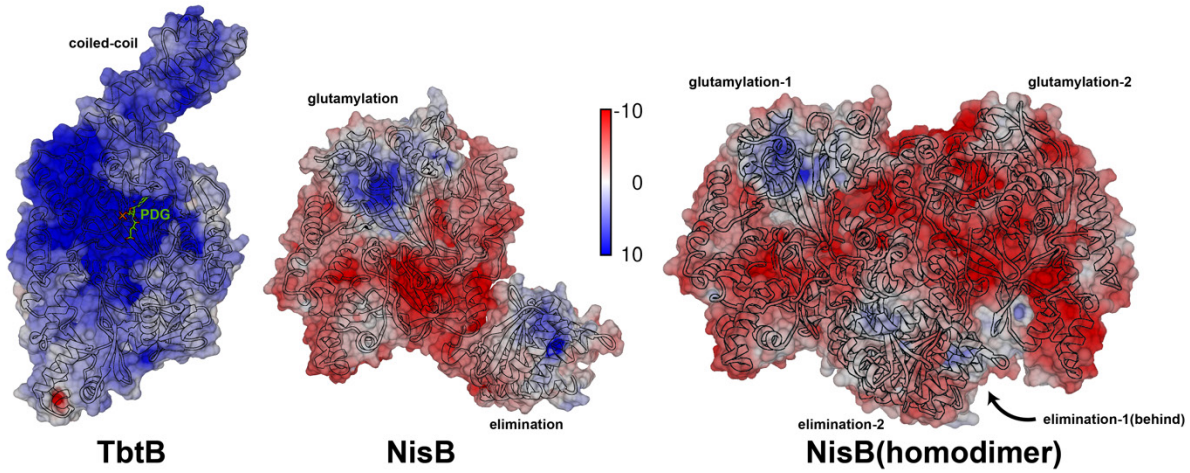

SI Appendix Figure 3: Electrostatic potential maps of TbtB, NisB (monomer), and NisB (homodimer) generated using PDB2PQR and the Adaptive Poisson-Boltzmann Solver (APBS) functionalities in UCSF Chimera 1.13 (5–7). TbtB and NisB were first superimposed and then separated (without rotation) for surface clarity.

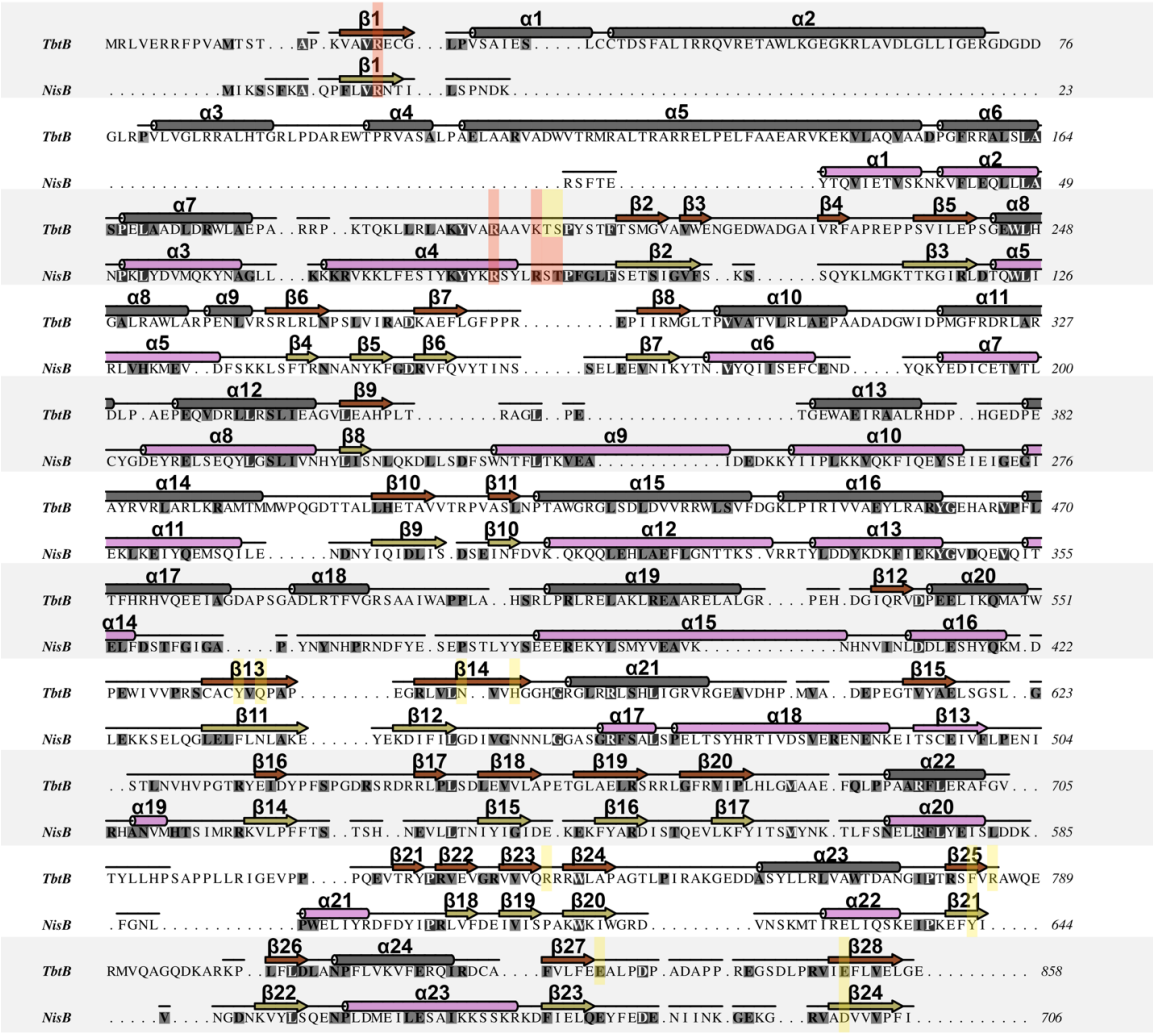

SI Appendix Figure 4: Structure-based multiple sequence alignment of $NisB_{1\text{-}706}$ and TbtB generated by PROMALS3D (25). Residues targeted for mutagenesis which gave partial or no impairment to activity are highlighted in yellow, and residues critical for activity are highlighted in red (SI Appendix Figures 6-7 and Tables 1-2) (3). For TbtB, helices are shown in dark gray, β-strands in brown, and random coils in light gray. For NisB, helices are shown in green, β-strands in khaki, and random coils in light gray.

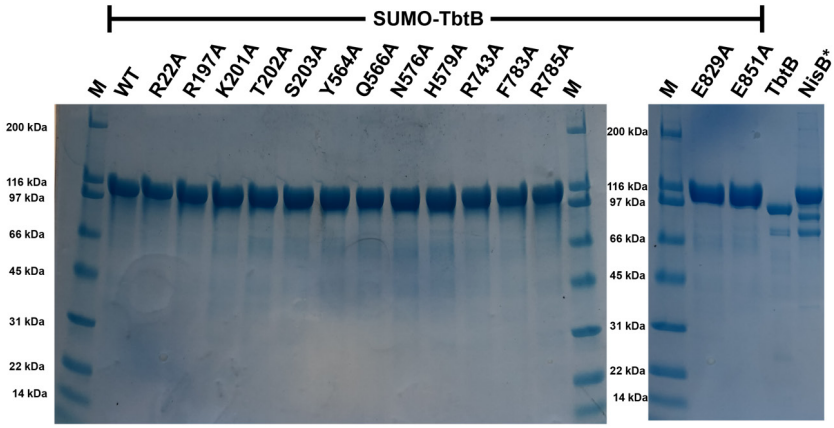

SI Appendix Figure 5: SDS-PAGE analysis of N-terminal His_6-SUMO tagged TbtB (SUMO-TbtB) variants (left panel) used in activity assays (SI Appendix Figure 6). Right panel, tag-free TbtB and methylated His_6-SeMet-NisB-V169C (NisB*) used for crystallization. "M" denotes protein standards.

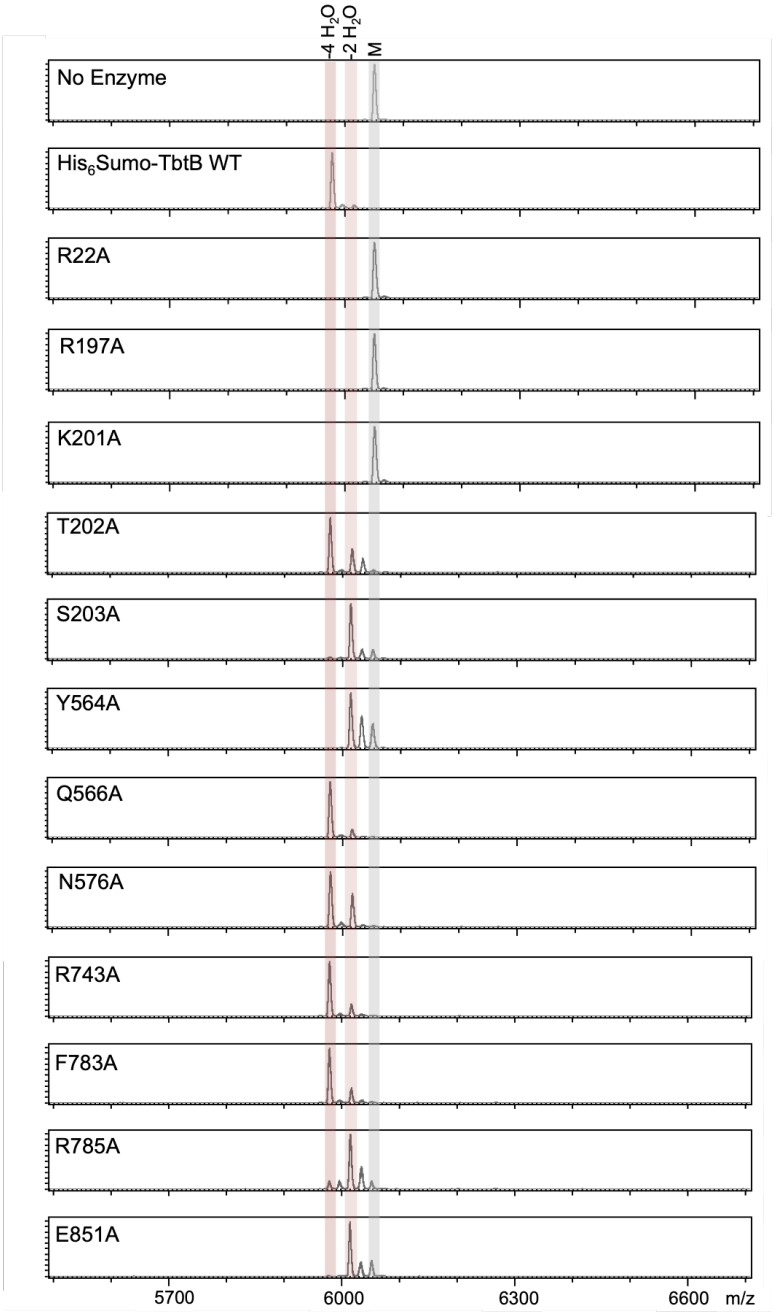

SI Appendix Figure 6: TbtB mutant activity. A panel of TbtB mutants selected via structure-guided analysis were expressed, purified by Ni-NTA affinity chromatography, and examined for activity *in vitro*. Reactions contained TbtB mutants, TbtC, GluRS, and $tRNA^{Glu}$ as described in the methods section and in previous reports (18) to allow for the dehydration of the TbtA-hexazole substrate. All reactions were incubated for 1 hour at room temperature prior to analysis by MALDI-TOF-MS. Wild-type (WT) TbtB was capable of fully dehydrating the TbtA hexazole substrate (−4 H_2O), whereas several mutants displayed decreased dehydration activity (−1 to −2 H_2O). Residues essential for enzyme function display no dehydration activity as evidenced by comparison to WT and no-enzyme controls.

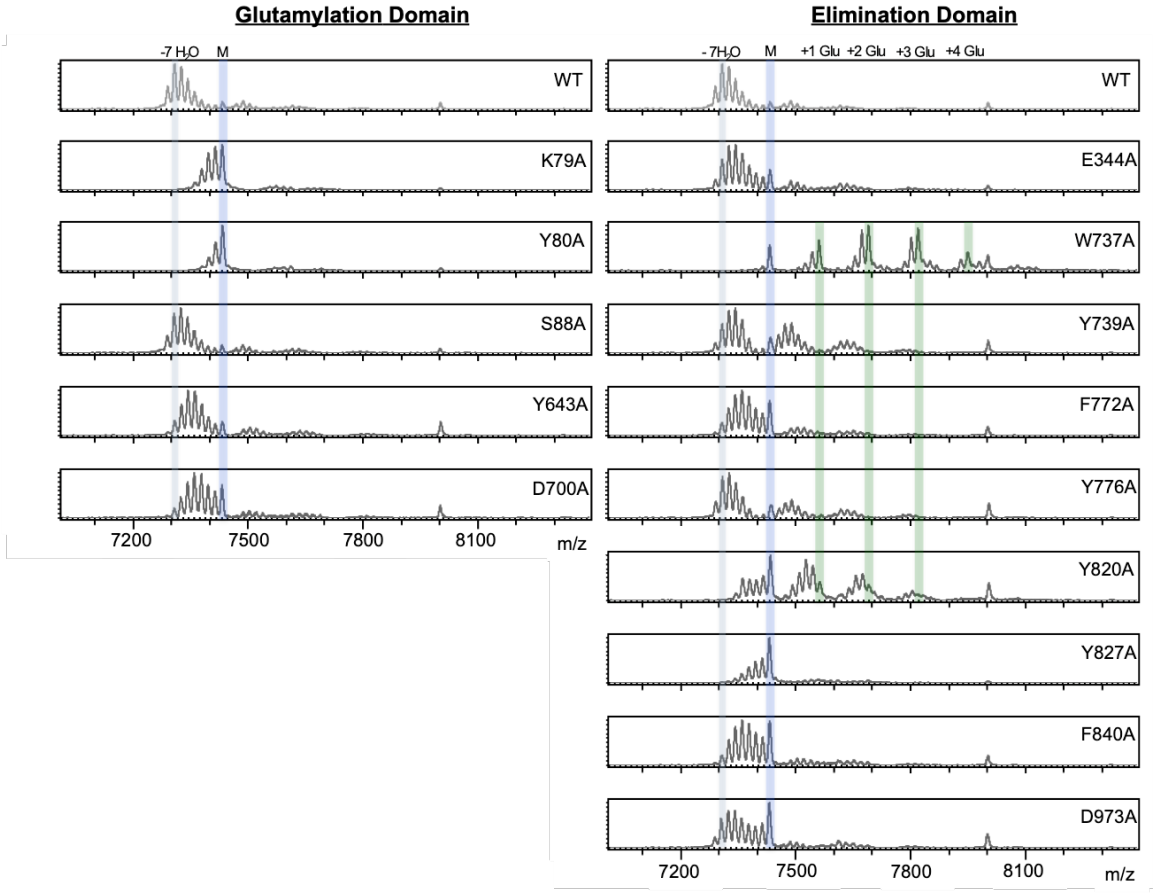

SI Appendix Figure 7: Structure-guided mutagenesis of NisB. His_6-NisA was coexpressed with NisB or its variants in *E. coli* BL21 Star (DE3) (26). Modified peptides were purified by Ni-NTA affinity chromatography and analyzed by MALDI-TOF MS. Left column, His_6-NisA coexpressed with glutamylation-domain variants of NisB. Diminished dehydration activity indicates the importance of Lys79 and Tyr80 for glutamylation. Right column, His_6-NisA coexpressed with elimination-domain variants of NisB. A build-up of glutamylated-peptide intermediates accompanied by diminished dehydration suggests the importance of key structural aromatic residues in the elimination domain.

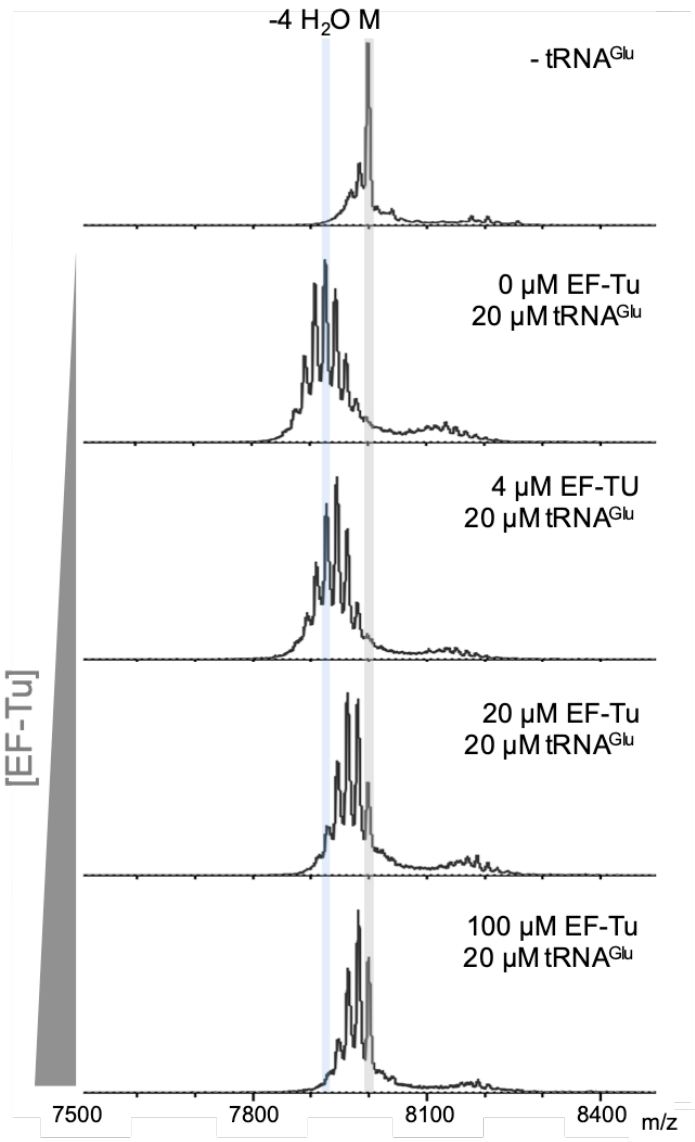

SI Appendix Figure 8: Effect of *E. coli* EF-Tu on NisB-mediated dehydration of NisA. Dose-dependent inhibition of NisB activity by GTP-bound EF-Tu, pre-incubated with *E. coli* $tRNA^{Glu}$, as analyzed by MALDI-TOF MS. The negative impact of EF-Tu on NisB activity suggests sequestration of the glutamyl-$tRNA^{Glu}$ cosubstrate.

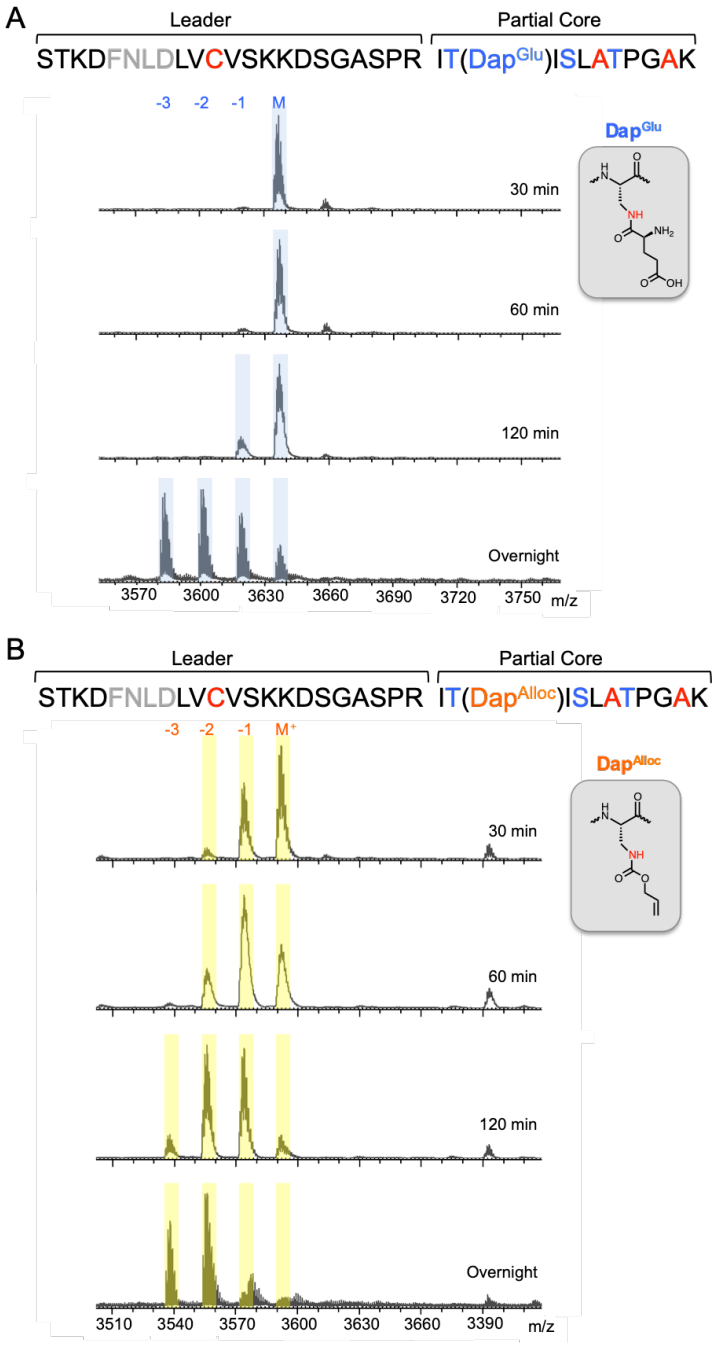

SI Appendix Figure 9: Dehydration of NisA analogues by wild type NisB. Time-course experiments monitoring the rate of dehydration of (A) NisA-Ser3Dap^{Glu} and (B) NisA-Ser3Dap^{Alloc} by NisB analyzed by MALDI-TOF MS. The dehydration of NisA-Ser3Dap^{Alloc} proceeds more rapidly than dehydration of the NisA-Ser3Dap^{Glu} peptide. The peptide sequences are colored according to key residues or amino acid substitutions. RRE-binding motif (FNLD), grey; Ser−12Cys, red; Cys7Ala and Cys11Ala, red; Dehydratable Ser/Thr in the core, blue; modified Ser+3Dap substitution, orange.

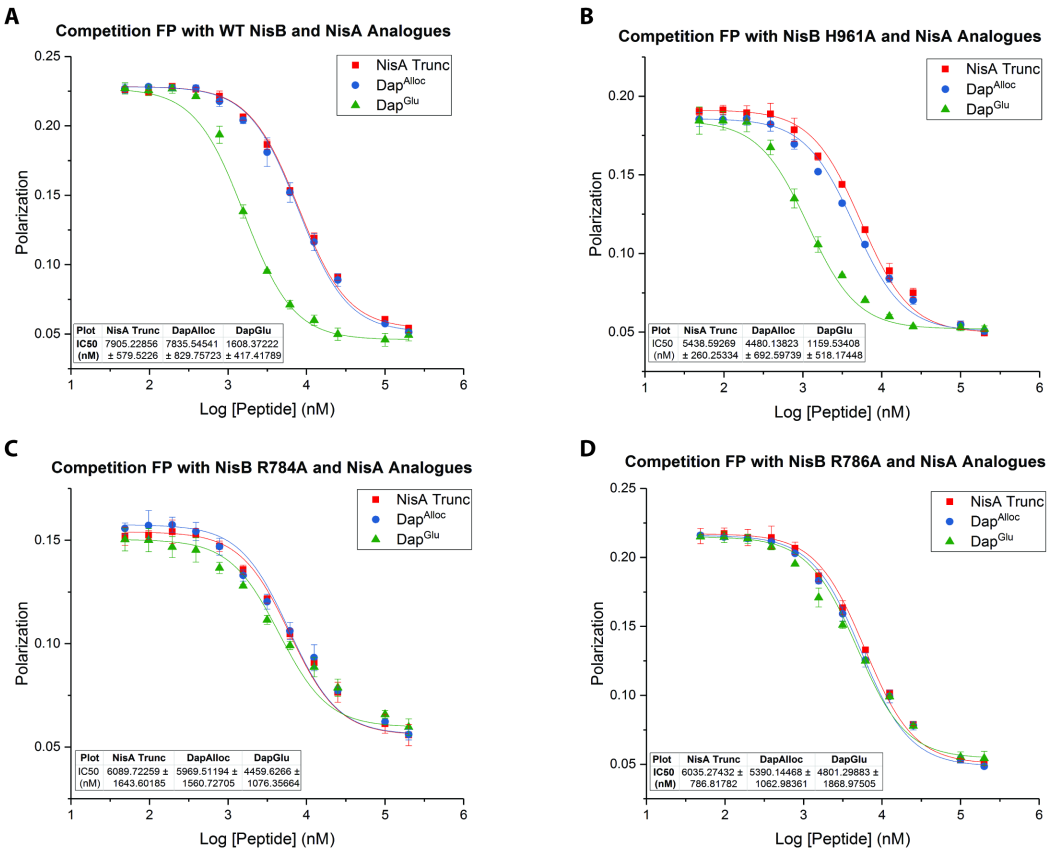

SI Appendix Figure 10: Examination of NisA-Ser3Dap^{Glu} binding. Competition fluorescence polarization assays using NisA-Ser3Dap^{Glu}, NisA-Ser3Dap^{Alloc}, or NisA-Trunc (see SI Appendix Scheme 2) to compete a FITC-NisA LP from wild-type NisB (A), NisB-H961A (B), NisB-R784A (C), or NisB-786A (D).

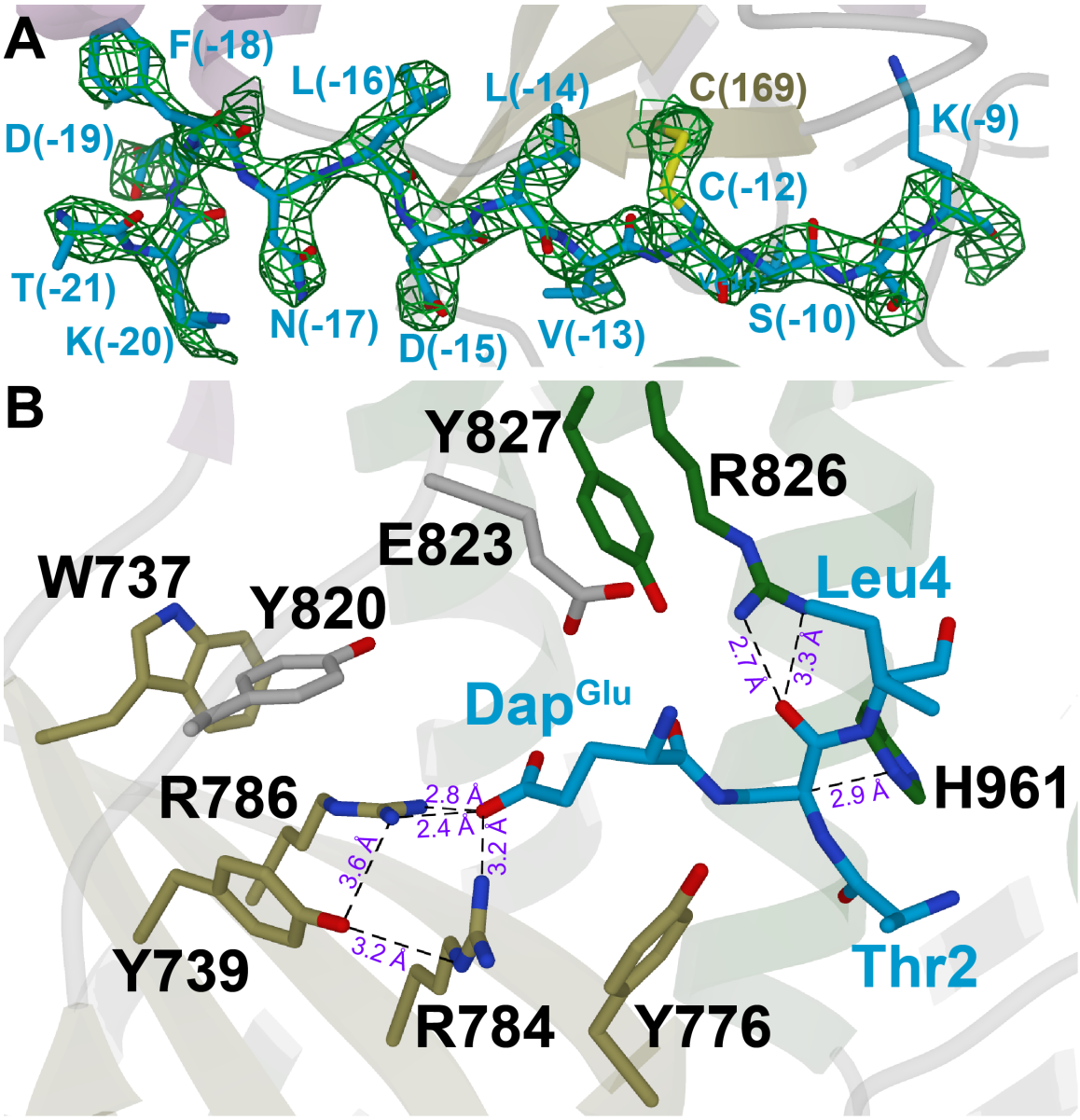

SI Appendix Figure 11: (A) Feature-enhanced map (FEM) (27) contoured at 1.8 σ is shown for residues −21 through −9 of NisA-Ser3Dap^{Glu}-Ser(−12)Cys bound at the RRE of NisB-Val169Cys including the engineered disulfide linkage between Cys(−12) of the peptide and Cys169 of NisB-Val169Cys (28). (B) NisB-V169C bound to NisA-Ser3Dap^{Glu} (2.79 Å; PDB 6M7Y) with additional residues shown as sticks (i.e. W737, Y739, and Y820) that showed significant attenuation in dehydration activity along with production of glutamylated adducts when mutated to Ala. Residues residing in an α-helix, β-sheet, or random coil are colored green, khaki, or light gray, respectively.

NMR data:

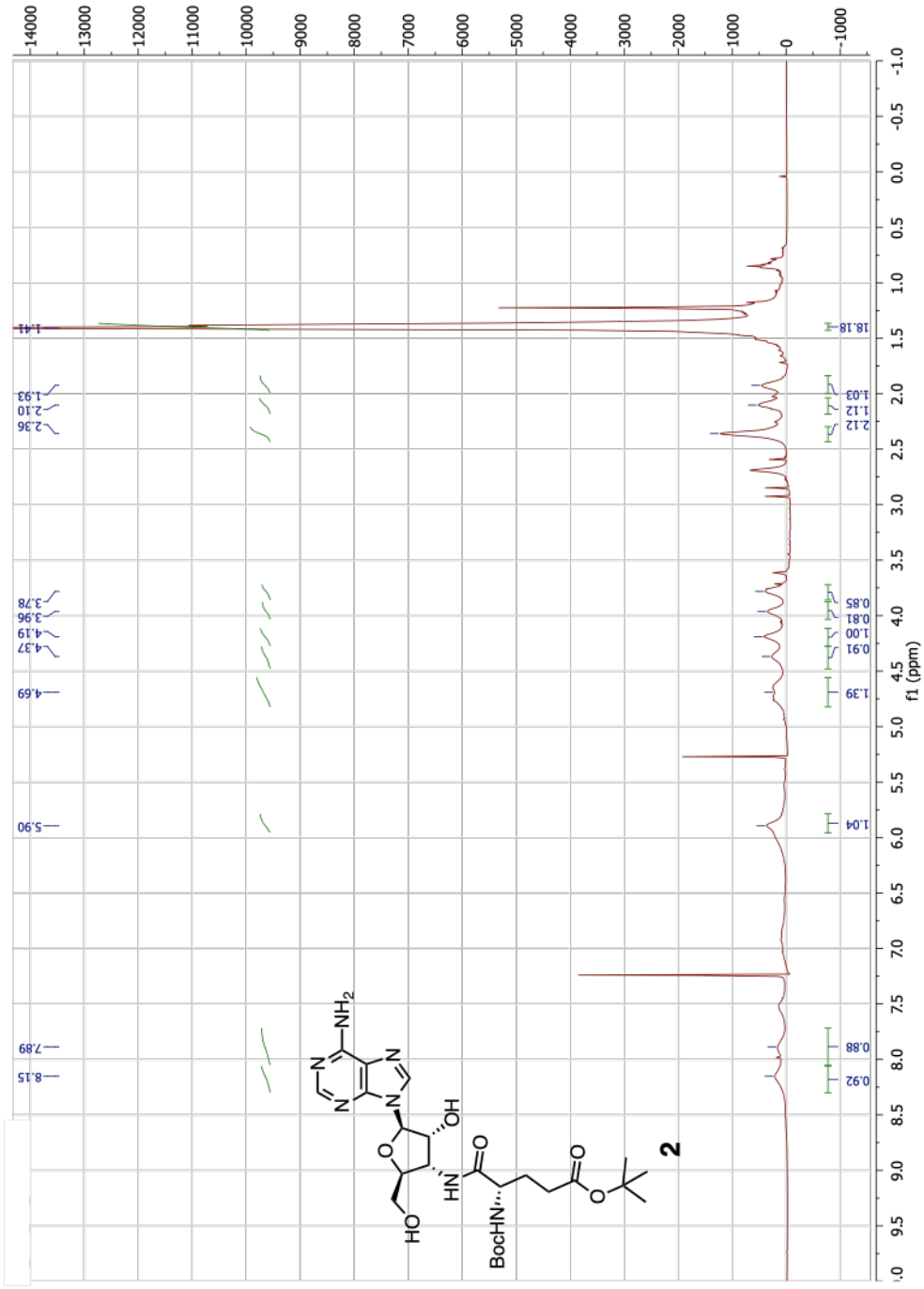

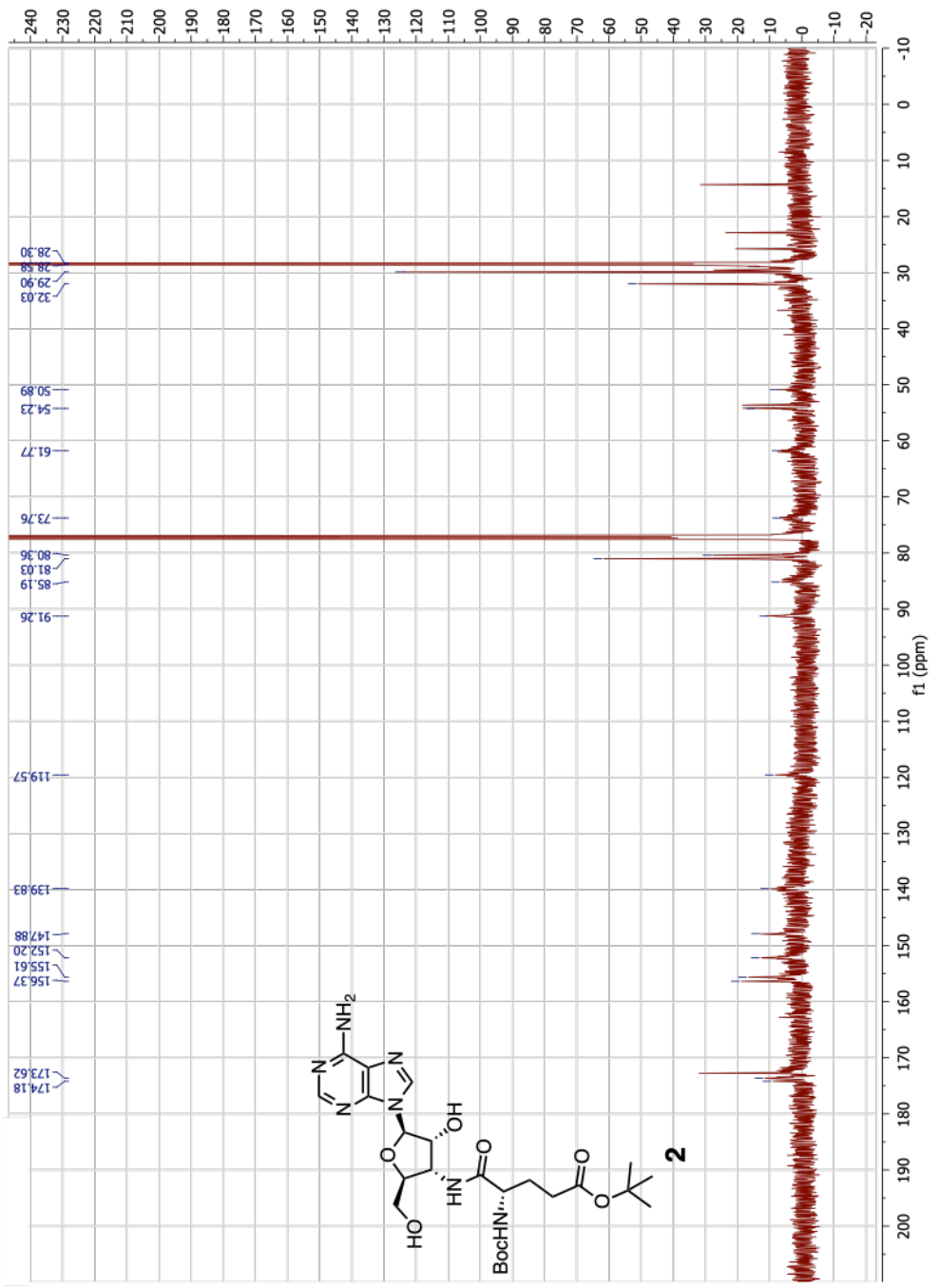
f1 (ppm)
28.30
28.58
29.90
32.03
50.89
54.23
61.77
73.76
80.36
81.03
85.19
91.26
119.57
139.83
147.88
152.20
155.61
156.37
173.62
174.18
NH2
OH
HO
NH
O
BocHN
2

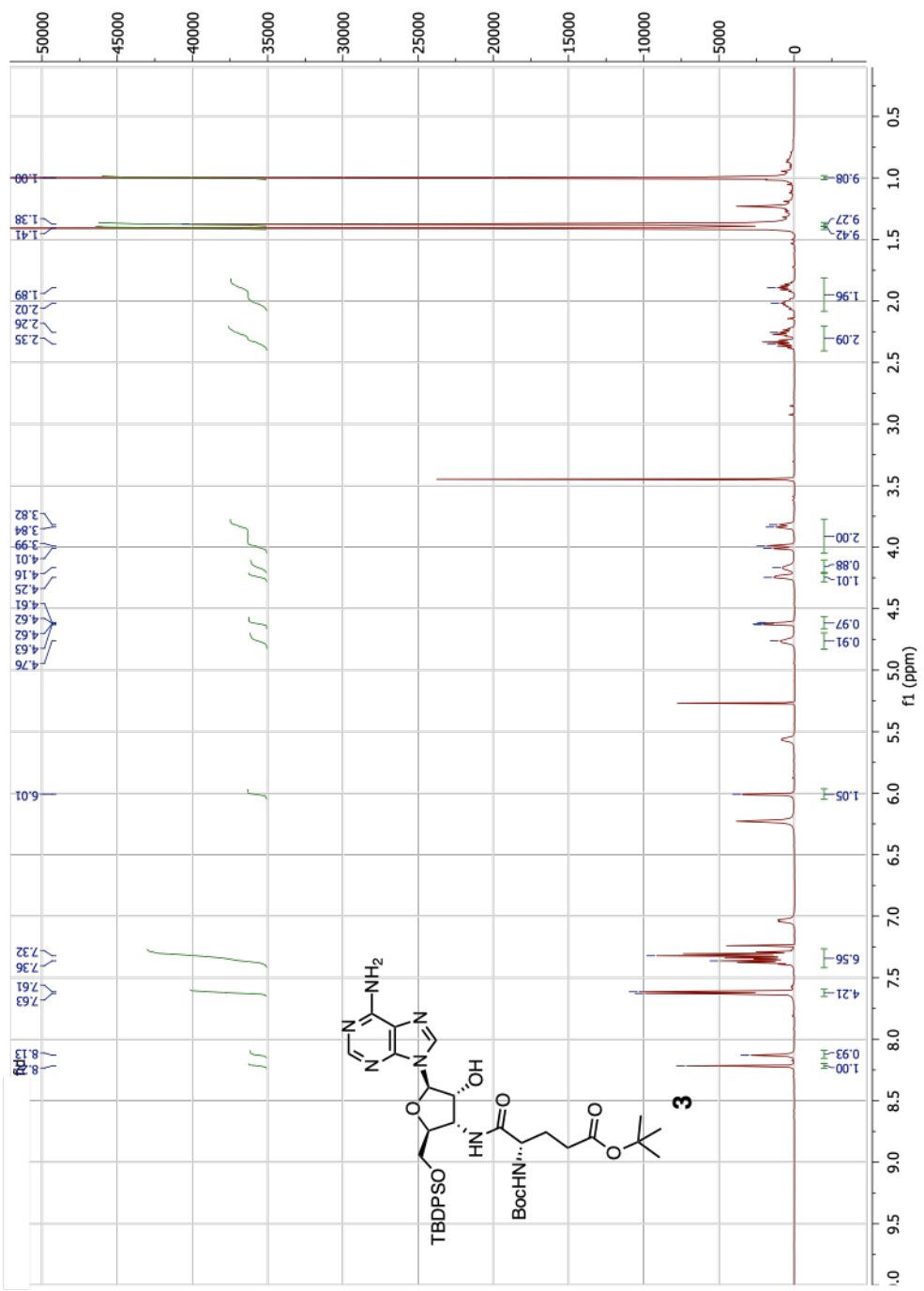
f1 (ppm)
TBDPSO
BocHN
HN
HO
NH2
3

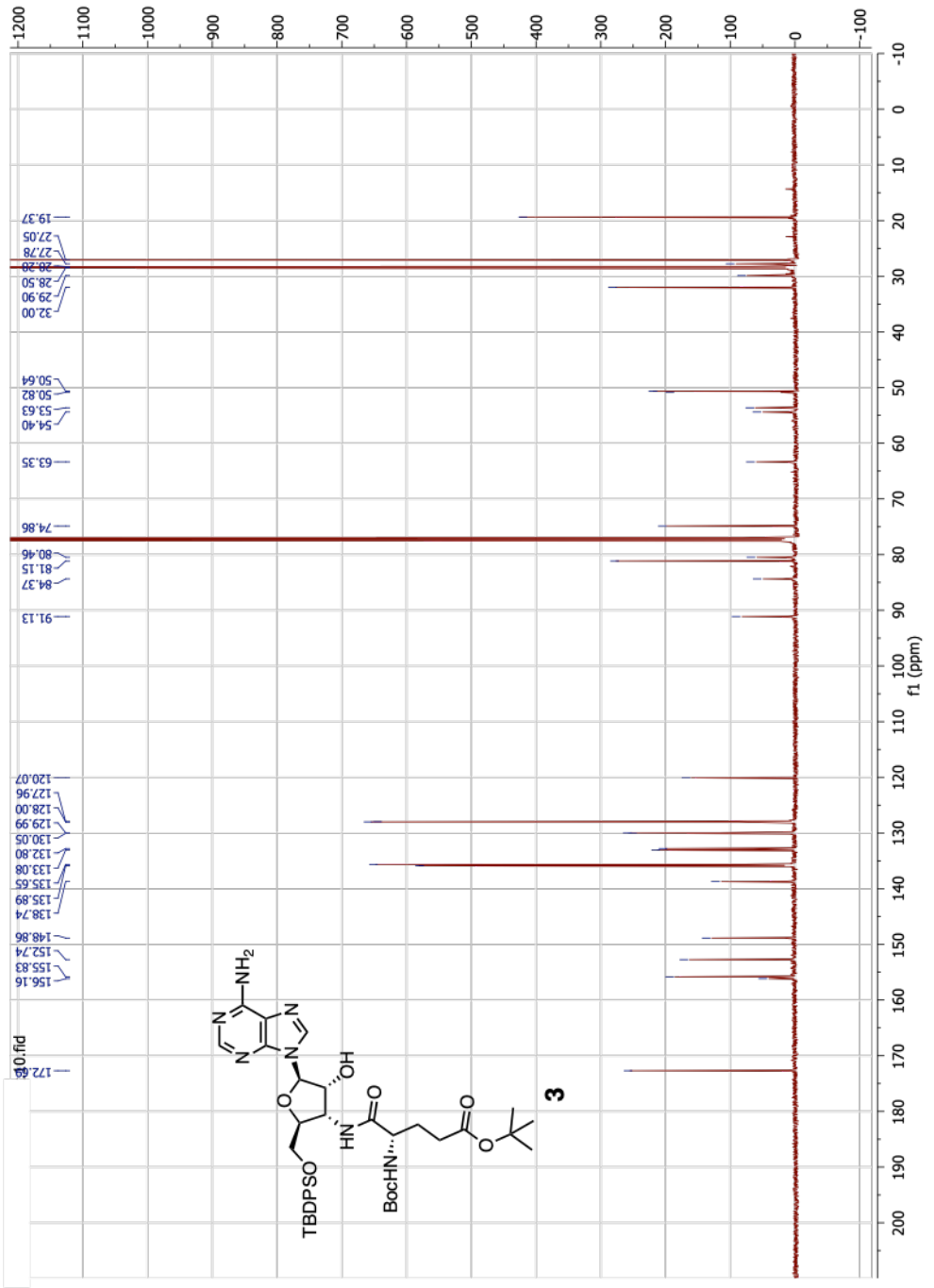
f1 (ppm)
TBDPSO
BocHN
HN
HO
NH2
3

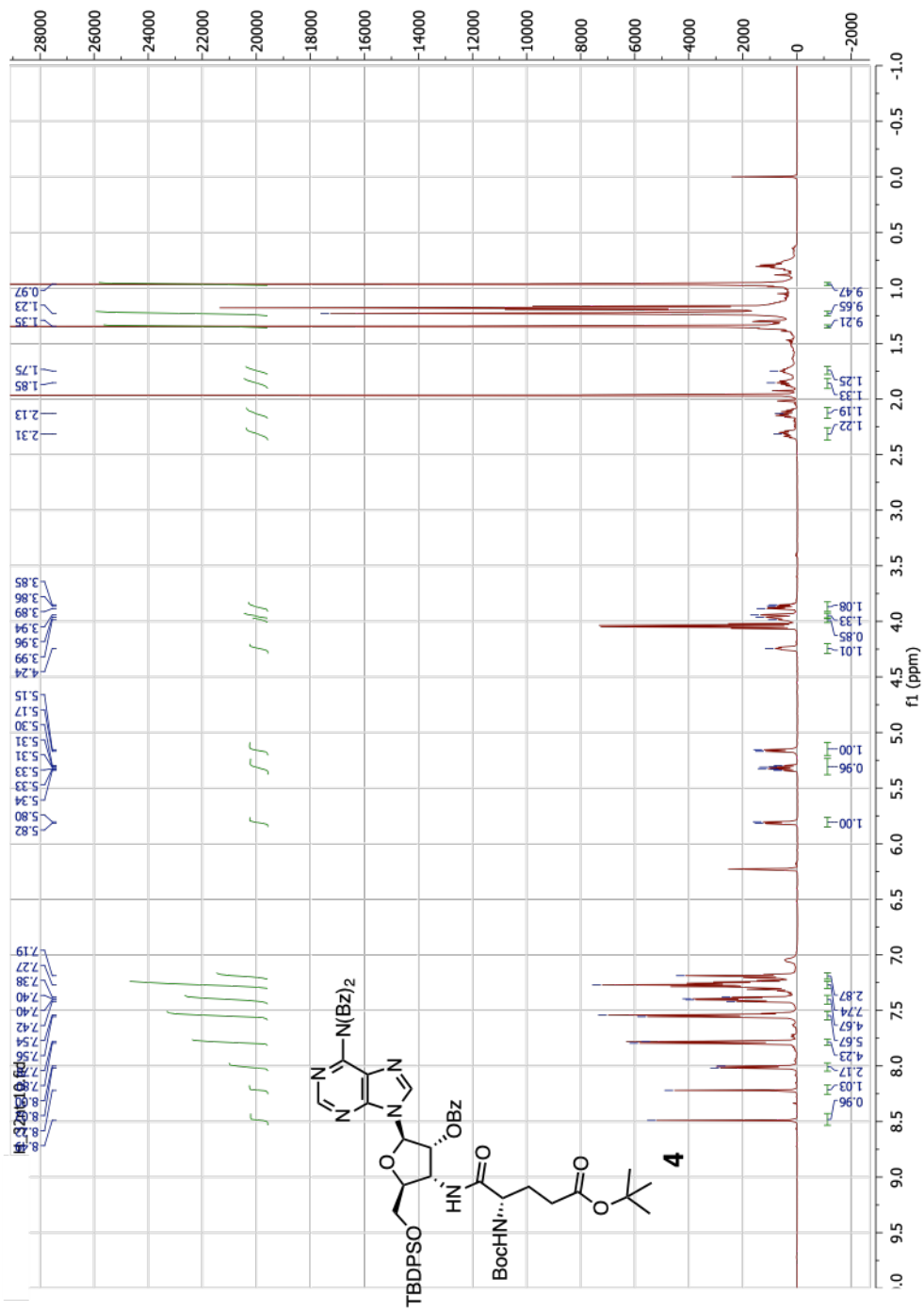
N(Bz)2
OBz
HN
BocHN
TBDPSO
4
f1 (ppm)

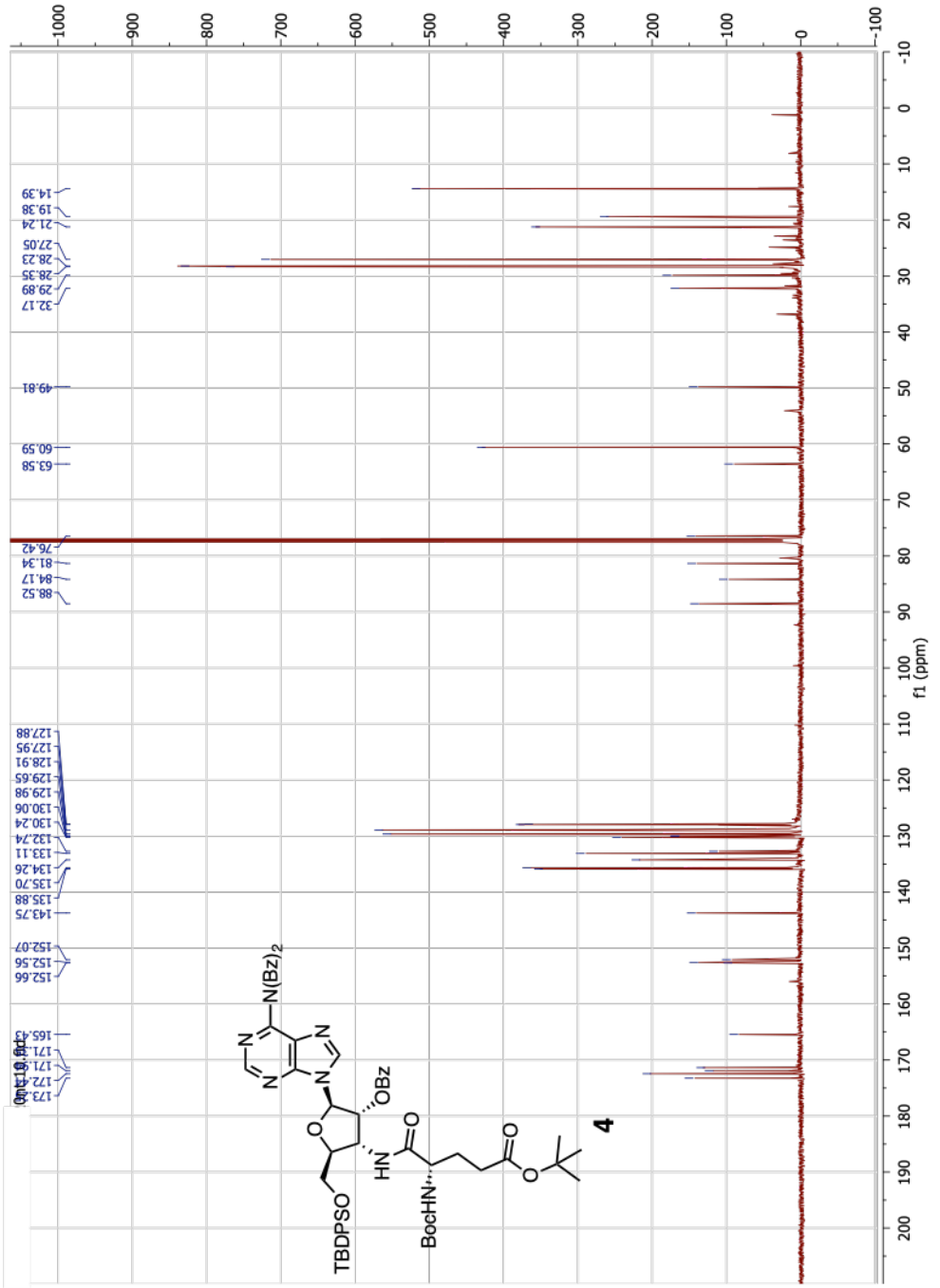
f1 (ppm)
N(Bz)2
OBz
HN
BocHN
TBDPSO
4

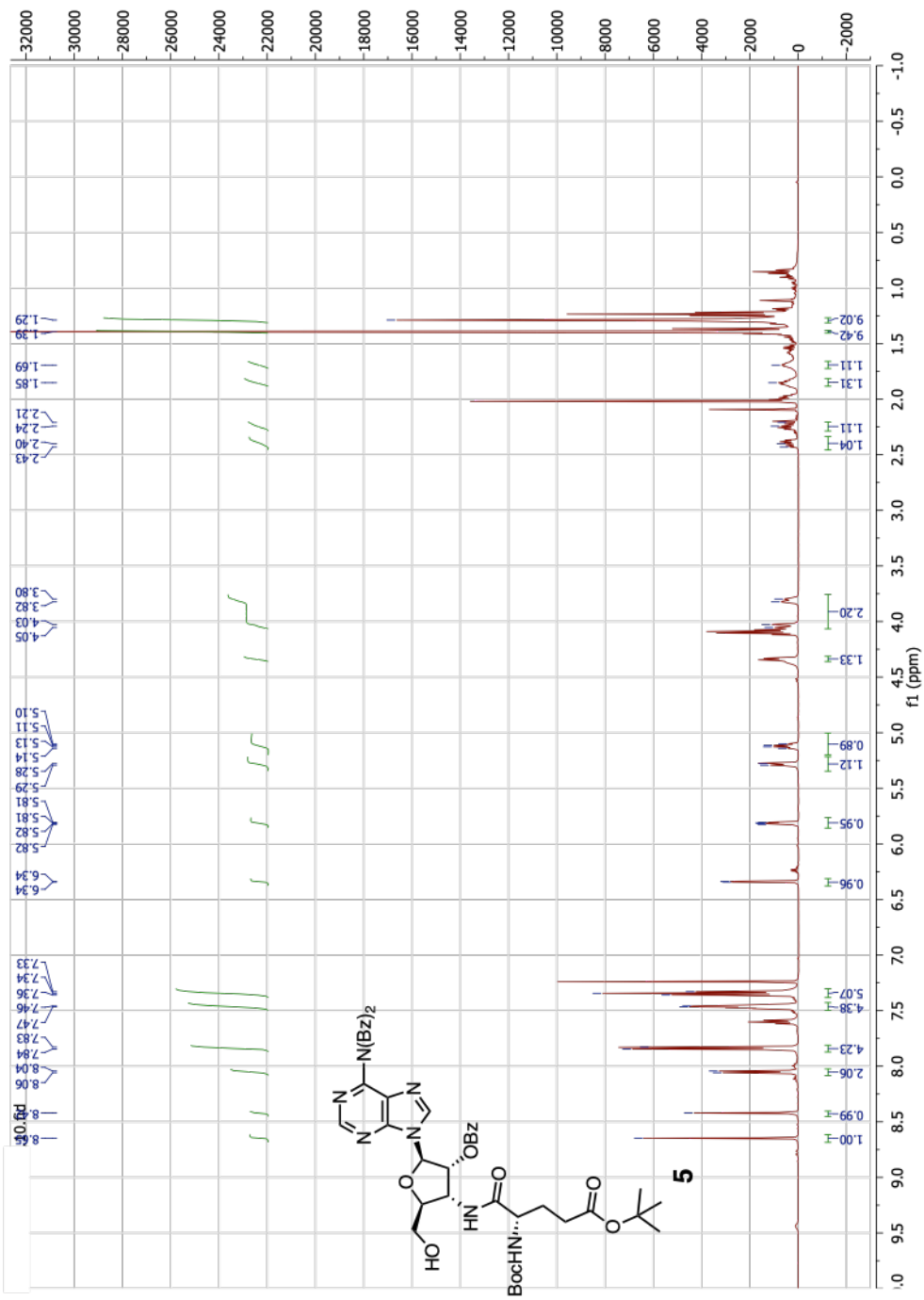
f1 (ppm)
N(Bz)2
OBz
HN
BocHN
OH
5

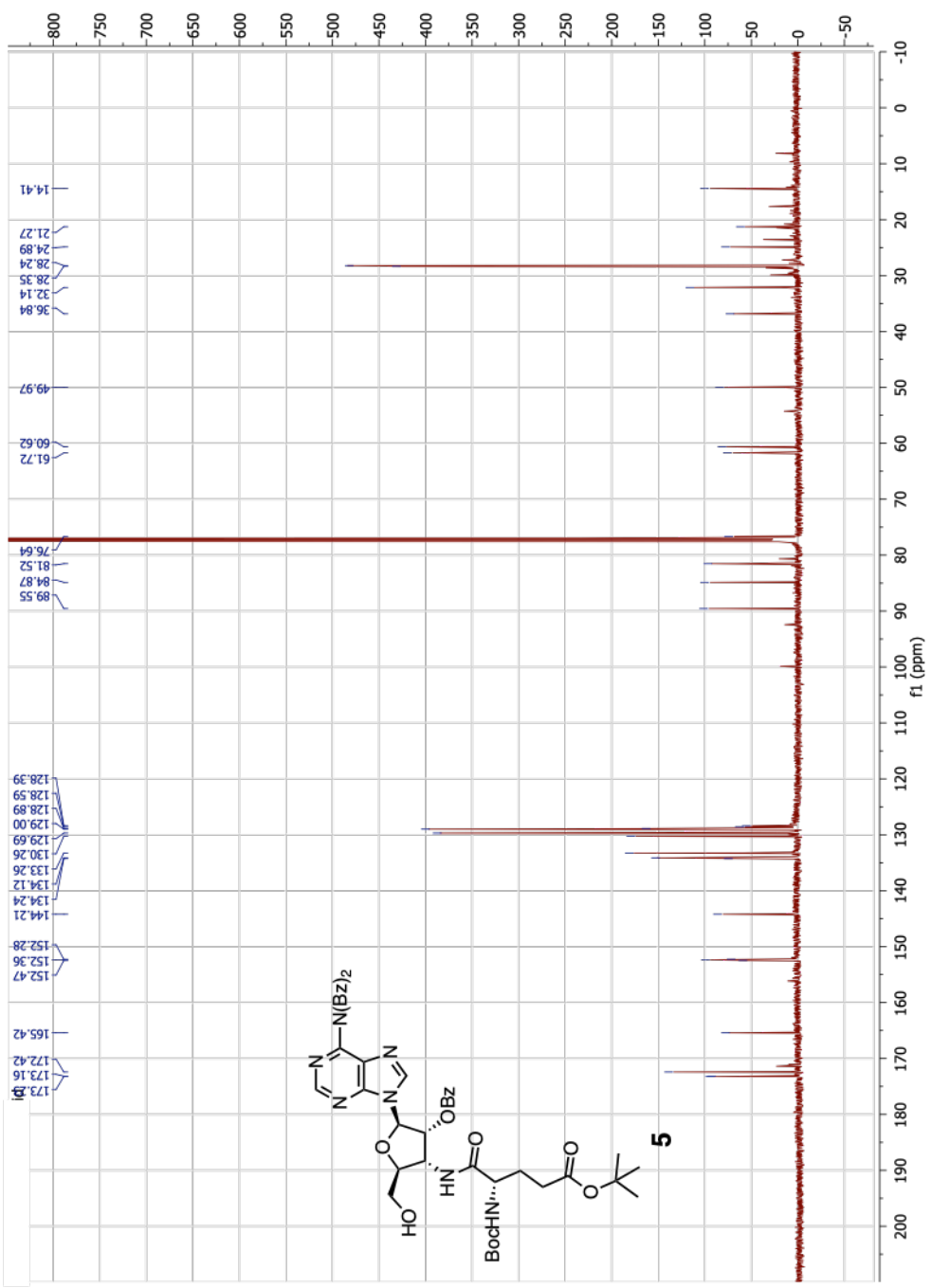
14.41
21.27
24.89
28.24
28.35
32.14
36.84
49.97
60.62
61.72
76.64
81.52
84.87
89.55
128.39
128.59
128.89
129.00
129.69
130.26
133.26
134.12
134.24
144.21
152.28
152.36
152.47
165.42
172.42
173.16
173.21
N(Bz)2
OBz
HO
HN
BocHN
O
O
O
5
f1 (ppm)

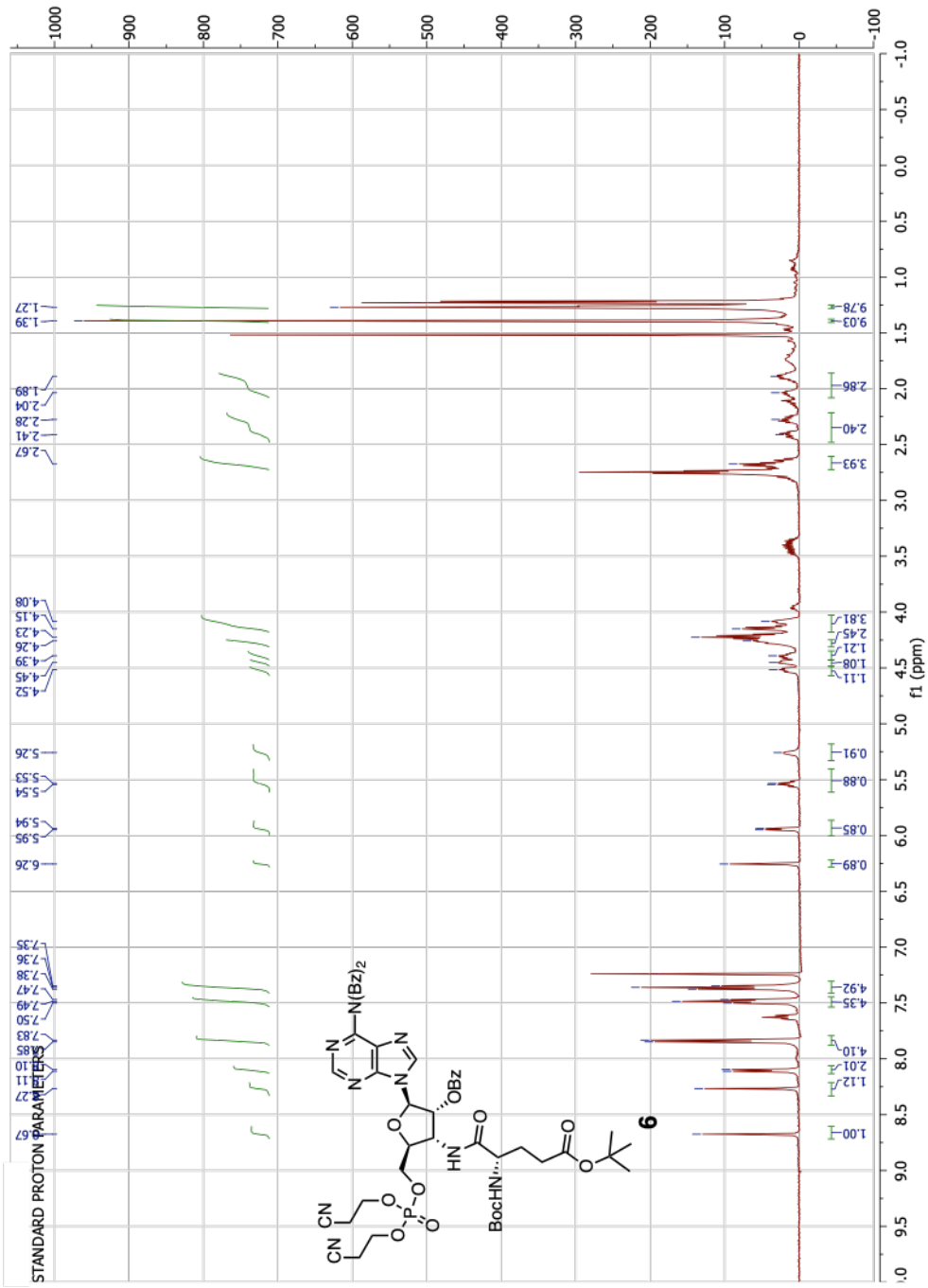
STANDARD PROTON PARAMETERS
f1 (ppm)
N(Bz)2
OBz
HN
BocHN
CN
CN
6

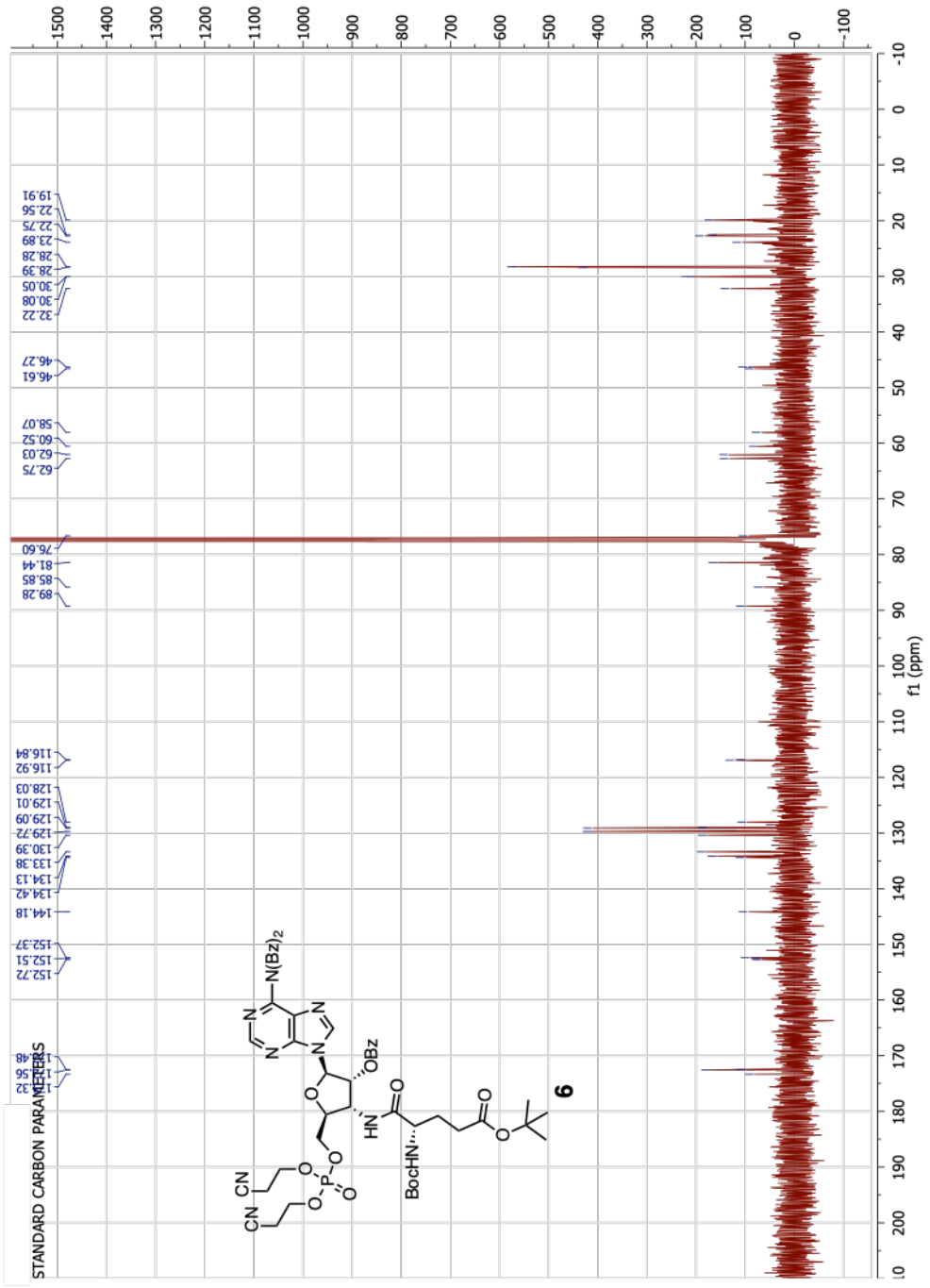
STANDARD CARBON PARAMETERS
19.91
22.56
22.75
23.89
28.28
28.39
30.05
30.08
32.22
46.27
46.61
58.07
60.52
62.03
62.75
76.60
81.44
85.85
89.28
116.84
116.92
128.03
129.01
129.09
129.72
130.39
133.38
134.13
134.42
144.18
152.37
152.51
152.72
N(Bz)2
OBz
HN
BocHN
CN
CN
6
f1 (ppm)

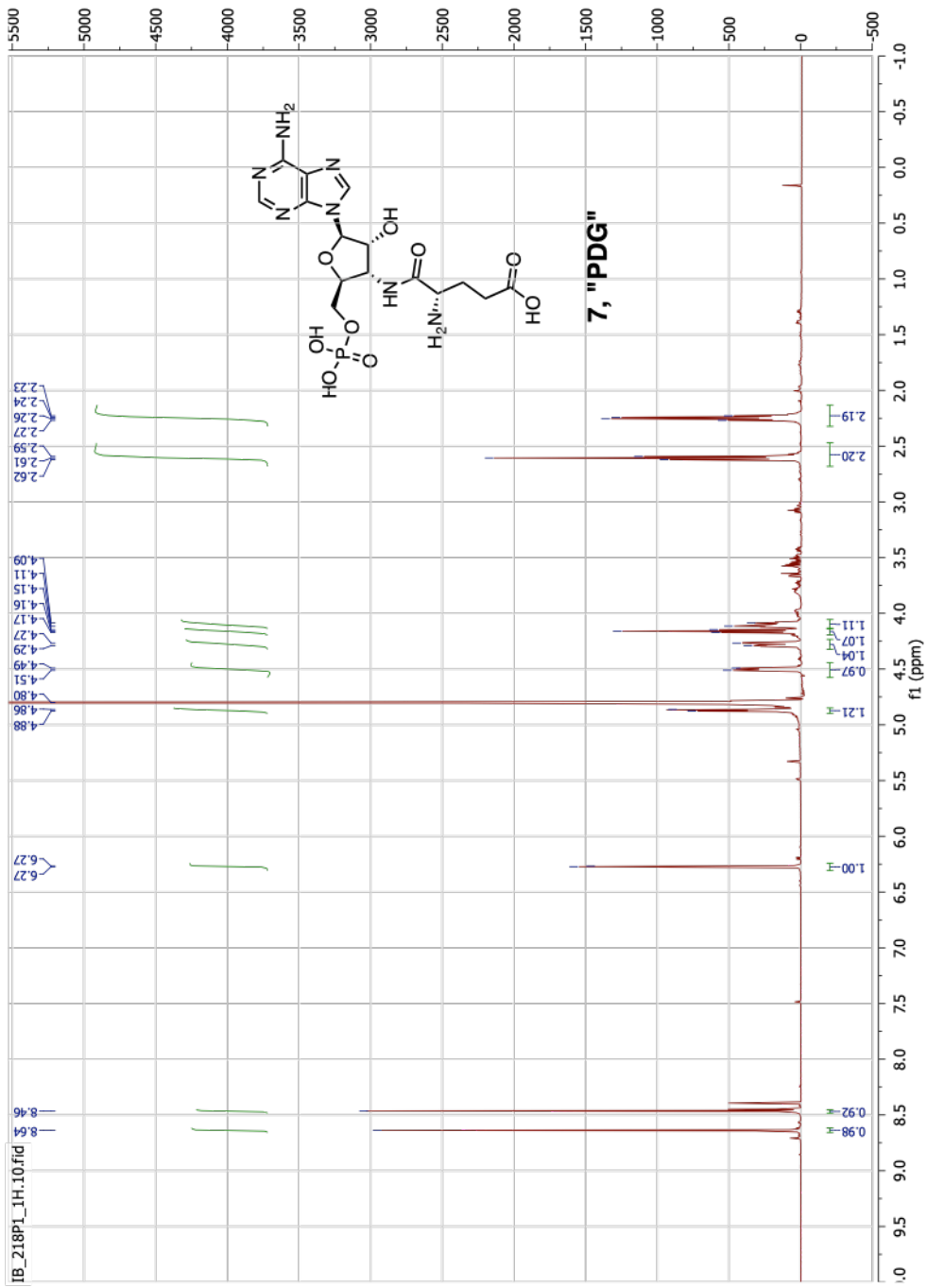
7, "PDG"
IB_218P1_1H.10.fid
f1 (ppm)

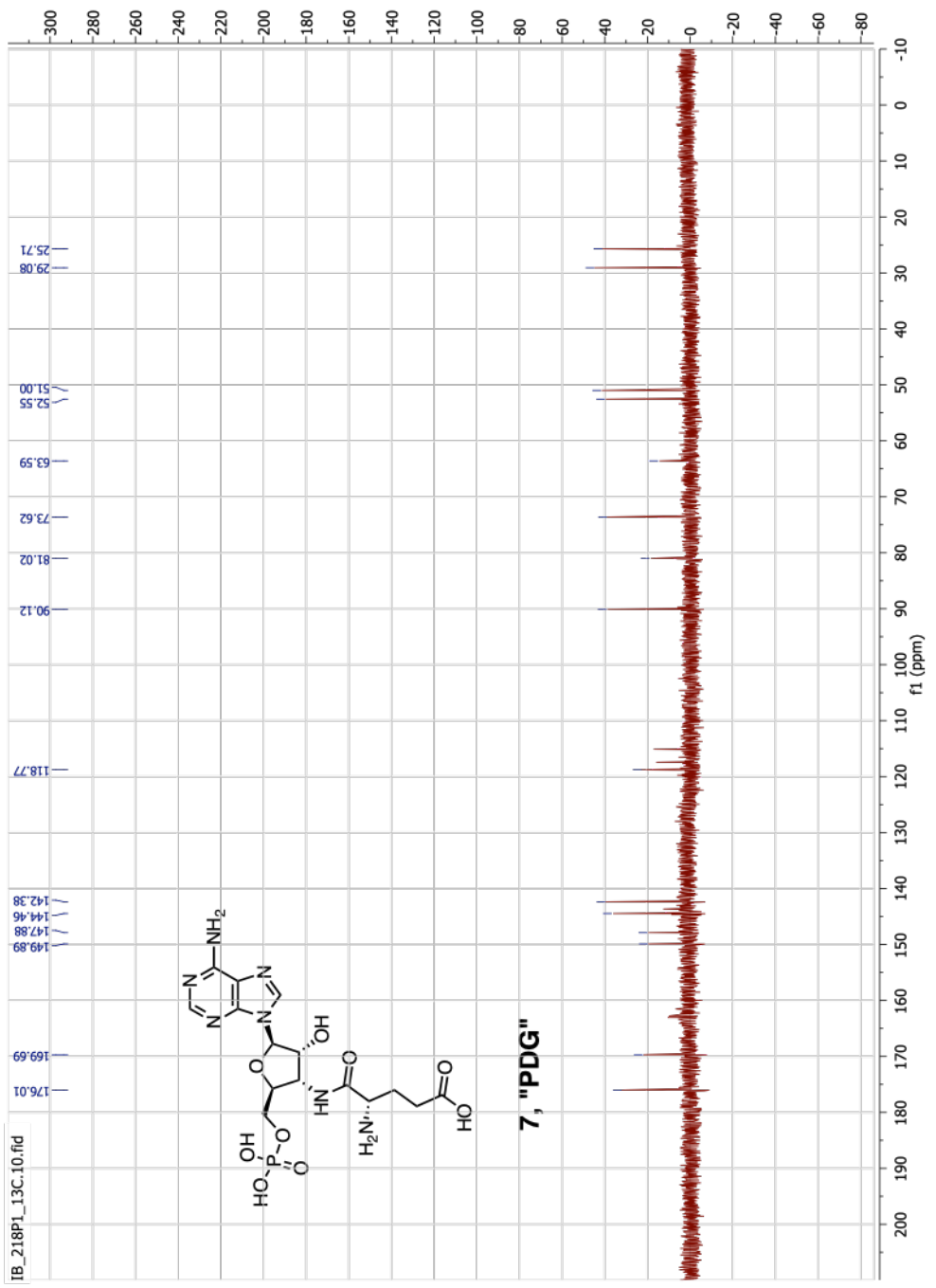
IB_218P1_13C.10.fid
7, "PDG"
f1 (ppm)
176.01
169.69
149.89
147.88
144.46
142.38
118.77
90.12
81.02
73.62
63.59
52.55
51.00
29.08
25.71

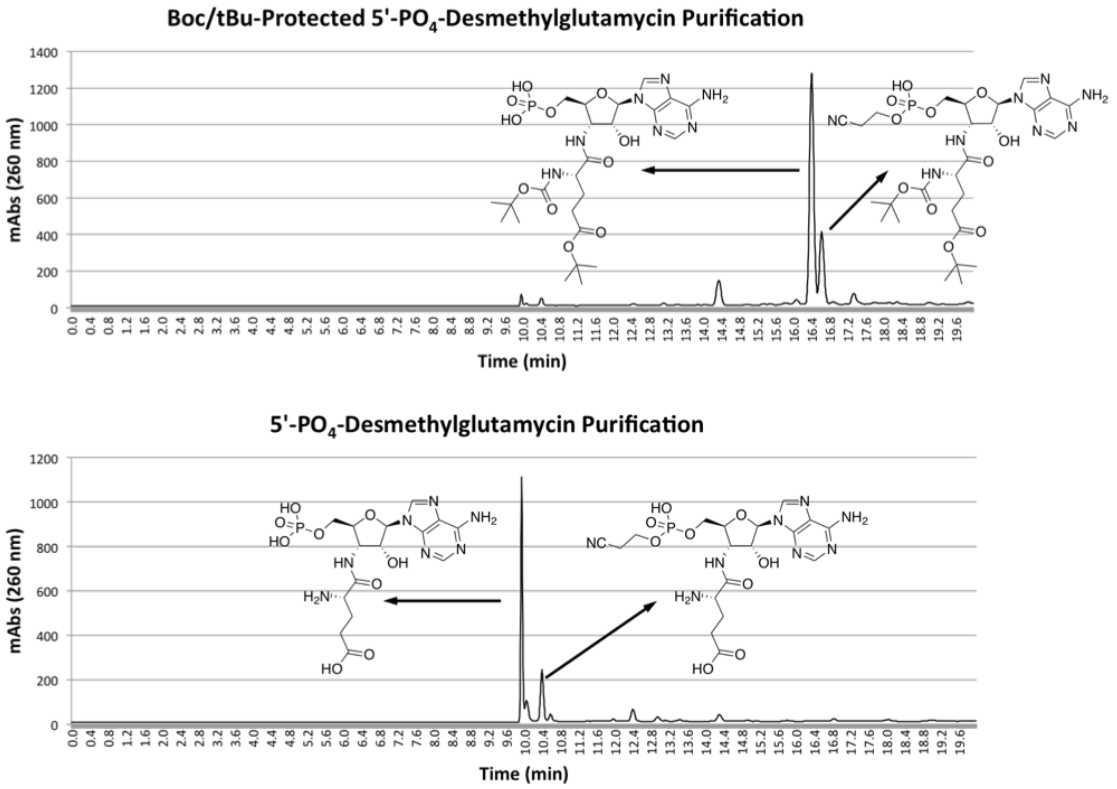

SI Appendix Figure 12: HPLC purification of PDG. Top panel, NH_4OH-treated **7** was analyzed by HPLC for comparison to final product. Bottom panel, NH_4OH-treated **7** was further deprotected by treatment with TFA and purified by HPLC.

Supporting References

1. Niedermeyer TH & Strohalm M (2012) mMass as a software tool for the annotation of cyclic peptide tandem mass spectra. *PLoS One* 7(9):e44913.
2. Gibson DG*, et al.* (2009) Enzymatic assembly of DNA molecules up to several hundred kilobases. *Nat. Methods* 6(5):343-345.
3. Garg N, Salazar-Ocampo LM, & van der Donk WA (2013) In vitro activity of the nisin dehydratase NisB. *Proc. Natl. Acad. Sci. U. S. A.* 110(18):7258-7263.
4. Chiu J, March PE, Lee R, & Tillett D (2004) Site-directed, Ligase-Independent Mutagenesis (SLIM): a single-tube methodology approaching 100% efficiency in 4 h. *Nucleic Acids Res.* 32(21):e174.
5. Li B, Cooper LE, & van der Donk WA (2009) In vitro studies of lantibiotic biosynthesis. *Methods Enzymol.* 458:533-558.
6. Vorstenbosch EL, Potapov AP, de Graaf JM, & Kraal B (2000) The effect of mutations in EF-Tu on its affinity for tRNA as measured by two novel and independent methods of general applicability. *J. Biochem. Biophys. Methods* 42(1-2):1-14.

7. Ling J, Yadavalli SS, & M. I (2007) Phenylalanyl-tRNA synthetase editing defects result in efficient mistranslation of phenylalanine codons as tyrosine. *RNA* 13(11):1881-1886.
8. Walter TS*, et al.* (2006) Lysine methylation as a routine rescue strategy for protein crystallization. *Structure* 14(11):1617-1622.
9. Kabsch W (2010) Xds. *Acta Crystallogr. D.* 66(Pt 2):125-132.
10. Terwilliger TC*, et al.* (2009) Decision-making in structure solution using Bayesian estimates of map quality: the PHENIX AutoSol wizard. *Acta Crystallogr. D Biol. Crystallogr.* 65(Pt 6):582-601.
11. Vonrhein C*, et al.* (2011) Data processing and analysis with the autoPROC toolbox. *Acta Crystallogr. D Biol. Crystallogr.* 67(Pt 4):293-302.
12. Afonine PV*, et al.* (2012) Towards automated crystallographic structure refinement with phenix.refine. *Acta Crystallogr. D Biol. Crystallogr.* 68(Pt 4):352-367.
13. Emsley P, Lohkamp B, Scott WG, & Cowtan K (2010) Features and development of Coot. *Acta Crystallogr. D Biol. Crystallogr.* 66(Pt 4):486-501.
14. Vagin AA*, et al.* (2004) REFMAC5 dictionary: organization of prior chemical knowledge and guidelines for its use. *Acta Crystallogr. D Biol. Crystallogr.* 60(Pt 12 Pt 1):2184-2195.
15. Terwilliger TC*, et al.* (2008) Iterative model building, structure refinement and density modification with the PHENIX AutoBuild wizard. *Acta Crystallogr. D Biol. Crystallogr.* 64(Pt 1):61-69.
16. McCoy AJ (2007) Solving structures of protein complexes by molecular replacement with Phaser. *Acta Crystallogr. D Biol. Crystallogr.* 63(Pt 1):32-41.
17. Moriarty NW, Grosse-Kunstleve RW, & Adams PD (2009) electronic Ligand Builder and Optimization Workbench (eLBOW): a tool for ligand coordinate and restraint generation. *Acta Crystallogr. D Biol. Crystallogr.* 65(Pt 10):1074-1080.
18. Hudson GA, Zhang Z, Tietz JI, Mitchell DA, & van der Donk WA (2015) In vitro biosynthesis of the core scaffold of the thiopeptide thiomuracin. *J. Am. Chem. Soc.* 137(51):16012-16015.
19. Balg C, Huot JL, Lapointe J, & Chenevert R (2008) Inhibition of *Helicobacter pylori* Aminoacyl-tRNA amidotransferase by Puromycin Analogues. *J. Am. Chem. Soc.* 130(11):3264-3265.
20. Khusainov R, van Heel AJ, Lubelski J, Moll GN, & Kuipers OP (2015) Identification of essential amino acid residues in the nisin dehydratase NisB. *Front Microbiol.* 6:102.
21. Sievers F*, et al.* (2011) Fast, scalable generation of high-quality protein multiple sequence alignments using Clustal Omega. *Mol. Syst. Biol.* 7:539.
22. Edgar RC (2004) MUSCLE: multiple sequence alignment with high accuracy and high throughput. *Nucleic Acids Res.* 32(5):1792-1797.
23. Waterhouse A*, et al.* (2018) SWISS-MODEL: homology modelling of protein structures and complexes. *Nucleic Acids Res.* 46(W1):W296-w303.
24. Crooks GE, Hon G, Chandonia JM, & Brenner SE (2004) WebLogo: a sequence logo generator. *Genome Res.* 14(6):1188-1190.

25. Pei J, Kim BH, & Grishin NV (2008) PROMALS3D: a tool for multiple protein sequence and structure alignments. *Nucleic Acids Res.* 36(7):2295-2300.
26. Shi Y, Yang X, Garg N, & van der Donk WA (2011) Production of lantipeptides in *Escherichia coli*. *J. Am. Chem. Soc.* 133(8):2338-2341.
27. Afonine PV, *et al.* (2015) FEM: feature-enhanced map. *Acta Crystallogr. D Biol. Crystallogr.* 71(Pt 3):646-666.
28. Repka LM, Hetrick KJ, Chee SH, & van der Donk WA (2018) Characterization of leader peptide binding during catalysis by the nisin dehydratase NisB. *J. Am. Chem. Soc.* 140(12):4200-4203.